Science of the Total Environment 868 (2023) 161474

Contents lists available at ScienceDirect

Science of the Total Environment

journal homepage: www.elsevier.com/locate/scitotenv

Fine particulate matter and its chemical constituents' levels: A troubling environmental and human health situation in Karachi, Pakistan

Omosehin D. Moyebi [a,b,*], Zafar Fatmi [c], David O. Carpenter [d], Muhayatun Santoso [e], Azhar Siddique [f], Kamran Khan [g], Jahan Zeb [h], Mirza M. Hussain [a,b], Haider A. Khwaja [a,b]

[a] Department of Environmental Health Sciences, School of Public Health, University at Albany, Albany, NY, USA
[b] Wadsworth Center, New York State Department of Health, Albany, NY, USA
[c] Environmental-Occupational Health & Climate Change Section, Department of Community Health Sciences, The Aga Khan University, Karachi, Pakistan
[d] Institute for the Health and the Environment, University at Albany, Albany, NY, USA
[e] National Nuclear Energy Agency (BATAN), Bandung, Indonesia
[f] Qatar Environment and Energy Research Institute, Hamad Bin Khalifa University, Doha, Qatar
[g] Chemistry Department, University of Karachi, Karachi, Pakistan
[h] Department of Environmental and Health Research, The Custodian of the Holy Two Mosques Institute for Hajj and Umrah Research, Umm Al-Qura University, Makkah, Saudi Arabia

HIGHLIGHTS

- Karachi's air quality is extremely poor and presents a significant human health risks.
- $PM_{2.5}$, Pb, Ni, Cr, and As concentrations significantly exceeds the WHO guidelines.
- AQI, risk and health impact assessment indicate poor air quality that is unhealthy for the general population and related to an increased estimate of the number of expected deaths.
- Vehicular and industrial emissions, oil combustion, and urban dust/soil resuspension greatly contribute to the levels of $PM_{2.5}$, BC, metals, and major ions.

GRAPHICAL ABSTRACT

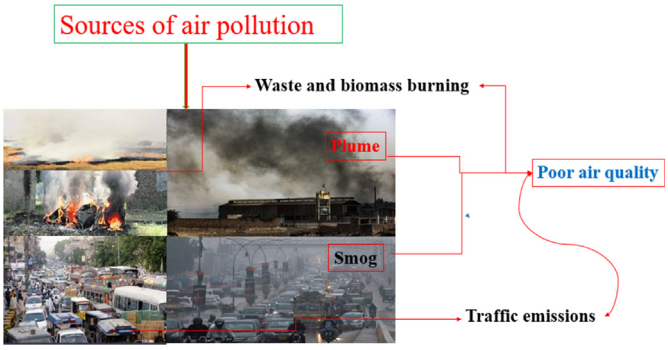

ARTICLE INFO

Editor: Jianmin Chen

Keywords:
Southeast Asia
$PM_{2.5}$
Black carbon
Metals
PMF

ABSTRACT

Like many urban centers in developing countries, the effect of air pollution in Karachi is understudied. The goal of this study was to determine the chemical characterization, temporal and seasonal variability, sources, and health impacts of fine particulate matter ($PM_{2.5}$) in Karachi, Pakistan. Daily samples of $PM_{2.5}$ were collected using a low-volume air sampler at two different sites (Makro and Karachi University) over the four seasons between October 2009 and August 2010. Samples were analyzed for black carbon (BC), trace metals, and water-soluble ions. Results showed that the annual average concentrations of $PM_{2.5}$ at Makro and Karachi University were 114 ± 115 and 71.7 ± 56.4 μg m^{-3}, respectively, about 22.8 and 14.3-fold higher than the World Health Organization annual guideline of 5 μg m^{-3}. BC concentrations were 3.39 ± 1.97 and 2.70 ± 2.06 μg m^{-3}, respectively. The concentrations of $PM_{2.5}$, BC, trace metals, and ions at the two sites showed clear seasonal trends, with higher concentrations in winter and lower concentrations in summer. The trace metals and ionic species with the highest concentrations were Pb, S, Zn, Ca, Si, Cl, Fe, and SO_4^{2-}. The air quality index in the fall and winter at both sites was about 68 %, which is "unhealthy" for the general population. Positive Matrix Factorization revealed the overall contribution to $PM_{2.5}$ at the Makro site came from three major sources – industrial emissions (13.3 %), vehicular emissions (59.1 %), and oil combustion (23.3 %). The estimates of expected number of deaths due to short-term exposure to $PM_{2.5}$ were high in the fall and winter at both sites, with an

* Corresponding author at: Department of Environmental Health Sciences, School of Public Health, University at Albany, Albany, NY, USA.
E-mail address: omoyebi@albany.edu (O.D. Moyebi).

http://dx.doi.org/10.1016/j.scitotenv.2023.161474
Received 27 June 2022; Received in revised form 2 January 2023; Accepted 4 January 2023
Available online 13 January 2023

annual mean estimate of 3592 expected number of deaths at the Makro site. Attention should be paid to the reduction of inorganic pollutants from industrial facilities, vehicular traffic, and fossil fuel combustion, due to their extremely high contribution to $PM_{2.5}$ mass and health risks.

1. Introduction

Air pollution is a global environmental problem of concern with >95 % of the world population living in areas with unhealthy air (State of Global Air, 2018; Pangaribuan et al., 2019). Premature deaths due to ambient and indoor air pollution across the world were estimated by the World Health Organization (WHO) to be about 4.2 million and 3.8 million, respectively, with 91 % of the deaths occur in developing countries (WHO, 2018; Lebbie et al., 2021). A 2014 United Nations' report estimated that about 66 % of the world's population will live in the cities by 2050 (Kumar et al., 2019). The growth in urban populations, traffic emissions, and industrial activities are the principal sources of global ambient air pollution (Simpson et al., 2014).

Developing countries in Southeast Asia such as Pakistan are witnessing an increase in air pollution due to increase in population, urbanization, industrial expansion, vehicular traffic, emerging economic growth, poor regulatory policies, road dust and motor vehicles with poor emission control (Tian et al., 2018; Ma et al., 2019; Lurie et al., 2019). A drastic increase in vehicular traffic as a result of population and economic growth in developing countries are contributing to the unhealthy levels of air pollutants (Cohen et al., 2010; Wu et al., 2017; Malashock et al., 2018). In fact, adequate air quality management systems are lacking in most developing countries due to poor legislation, political problems, and financial difficulties (Omanga et al., 2014; Zou et al., 2015). Economic development is of greater interest than air pollution mitigation or control in low-income countries (Omanga et al., 2014), which is one reason that air pollution is still a serious environmental issue and human health risk.

Epidemiological evidence has confirmed that air pollution exposure adversely impacts human health and aggravates health issues (Phosri et al., 2018; Xia et al., 2019; Rajak and Chattopadhyay, 2020; Soleimani et al., 2022). The International Agency for Research on Cancer (IARC) has classified particulate matter (PM) and outdoor air pollution as Group 1 agents, which have been proven to be carcinogenic to humans (IARC, 2016). Air pollution is also associated with cardiopulmonary problems resulting in increased healthcare cost, morbidity, and mortality (Pope and Dockery, 2013; Yang et al., 2019). According to State of Global Air rankings (2018), the top five countries with the highest mortality rate due to air pollution are all in Asia and include China, India, Pakistan, Indonesia, and Bangladesh. China and India together were responsible for more than half of the total early deaths attributable to ambient fine particulate matter ($PM_{2.5}$) in 2016 (State of Global Air, 2018).

Several studies on air pollution and its effects have primarily focused on developed countries (Khwaja et al., 2012), resulting in adequate environmental regulations. In contrast, developing countries in Southeast Asia remain adversely affected by air pollution. Gurung and Bell (2013) found that most of the recent air pollution studies in Asia often focused on a few cities leaving the larger population at the risk of poor air quality. More attention is needed for Southeast Asian countries such as Pakistan with exponential population growth i.e., an increase from 107 million in 1990 to 229 million in 2022 accompanied by enormous economic development and increasing sources of air pollution. Pakistan has witnessed an unprecedented increase in vehicular traffic. According to the Pakistan Bureau of Statistics, in only one year, the total number of vehicles in Pakistan increased by 9.6 % (23.59 million in 2018 compared to 21.51 million in 2017.

Karachi is the largest city in Pakistan, with an annual growth rate of 6 %. As the most affluent Pakistani city, Karachi is home to major industries as described in Khwaja et al. (2012) and Lurie et al. (2019), representing 30 % of country's manufacturing sectors (Barletta et al., 2002; Anjum et al., 2021). Currently, there are 4.14 million registered vehicles plying the roads of Karachi. According to a 2019 study that ranked 100 major cities, Karachi had the world's worst public transport system, with old and overcrowded buses serving approximately 42 % of the city's commuters (Bloomberg, 2020). Karachi is the only megacity which does not have the mass transit system. Open burning of municipal garbage and waste incineration are also a serious environmental problem in Karachi (Khwaja et al., 2012). In this and other major cities of Pakistan, comprehensive assessments of mass concentrations, chemical compositions, sources, and health risks of $PM_{2.5}$ are scarce, which limits the policy makers ability to implement appropriate pollution control measures. This study was designed to gather urgently needed information on $PM_{2.5}$ and its chemical constituents, spatial, temporal, and seasonal variability, sources, and health impacts in Karachi, Pakistan.

2. Materials and methods

2.1. Sampling sites

Karachi is a megacity in Pakistan with 18 towns (01-Baldia, 02-Bin Qasim, 03-Gadap, 04-Gulberg, 05-Gulshan, 06-Jamshed, 07-Kemari, 08-Korangi, 09-Landhi, 10-Liaquatabad, 11-Lyari, 12-Malir, 13-North Nazimabad, 14-New Karachi, 15-Orangi, 16-Saddar, 17-Shah Faisal, and 18-Sindh Industrial Trading Estate and 6 cantonments) (Fig. 1). It is located on the Arabian Sea (Lat. 24°51′ N; Long. 67°02′ E) (Khwaja et al., 2012; Lurie et al., 2019). Karachi has a population of 24 million residents (Moryani et al., 2020) accounting for almost 10 % of the country's total population with about 40 % of the residents living in low-income or squatter colonies and non-zoned settlements (Khwaja et al., 2012).

The climate condition in Karachi is subtropical with yearly rainfall averaging 256 mm, which mainly falls between July and August during the monsoon (Lurie et al., 2019). The Karachi landscape is characterized by flat or rolling plains with an extended coastal zone in the southeast and hills on the west and north (Khwaja et al., 2012). The city is about 58 % dry in the winter with December being the driest month and 85 % humid in summer with August being the wettest month (Lurie et al., 2019).

2.2. Sample collection and analysis

Daily samples of $PM_{2.5}$ were collected and chemically analyzed for pollutants (BC, trace metals, and water-soluble ionic species) at two different fixed sites over the four seasons of the year between October 2009 and August 2010. The sites were Karachi University (KU) (commercial/residential) and Makro (industrial/residential) (Fig. 1). Detailed $PM_{2.5}$ sample collection and data acquisition as well as the quality assurance/quality control (QA/QC) followed the methods described in Khwaja et al., 2012, Malashock et al., 2018, and Lurie et al., 2019.

2.2.1. Black carbon

A Dual-Wavelength Optical Transmissometer (Model OT-21, Magee Scientific Company, Berkeley, CA) at two wavelengths of 370 nm (BC_{UV}) and 880 nm (BC_{IR}) was used to measure the BC (Lurie et al., 2019). A set of blank filters was analyzed as a QC measure to estimate the variations between blanks and for instrument calibration. One of the possible markers for identifying biomass burning as the major source of BC is the difference between measured BC at the two different wavelengths (Delta-C = $BC_{370\ nm} - BC_{880\ nm}$) (Lurie et al., 2019).

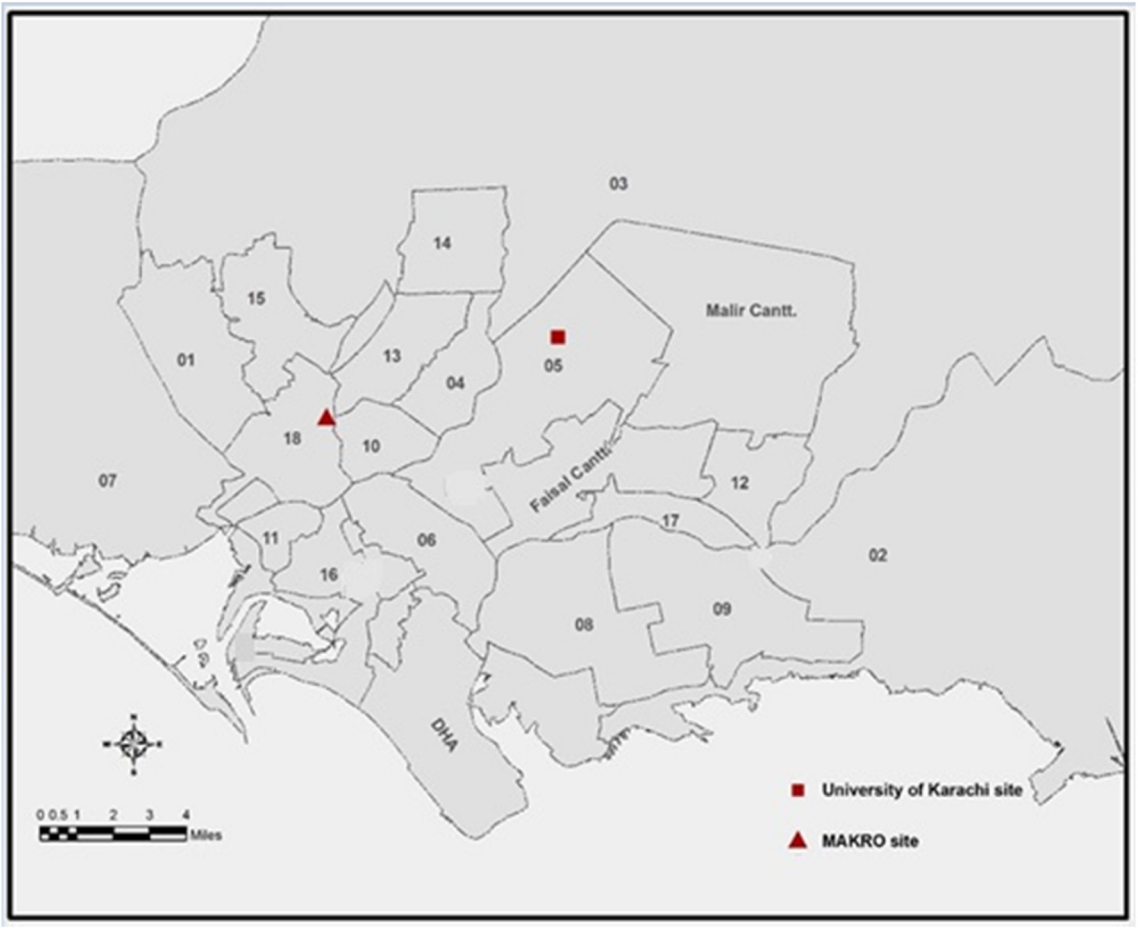

Fig. 1. Karachi map showing the sampling sites during the study period.

2.2.2. Trace metals

Trace metals were analyzed by nuclear techniques in addition to the Thermo Scientific ARL QUANTX energy dispersive X-ray fluorescence (EDXRF) spectrometer (Model AN41903-E 06/07C, Ecublens, Switzerland). The EDXRF spectrometer achieves a highly precise and reliable performance by concurrently measuring elemental concentration with the corresponding uncertainty (Lurie et al., 2019). The nuclear technique uses Instrumental Neutron Activation Analysis (INAA), which can determine various elements at low levels but cannot detect elements with short half-life (NIST, 2019). The ratio of each concentration measured to its uncertainty (> 3) was used to determine the validity of the obtained measurements. This study reported trace metals with concentrations above the limit of detection and those that were three times higher than the uncertainty values.

The QC was efficiently put in place by analyzing QC sample before and after each sequence with an energy (eV)-calibrated instruments for every batch of samples. Furthermore, the sample holders were thoroughly cleaned with deionized water from Barnstead Water Purification Systems (Thermo Fisher Scientific) for each analytical sequence to avert contamination. The field blank filters were analyzed as part of the QC measure and subtracted from the sample concentration to minimize contamination and overestimation. We used the exposed filter area (16.764 cm^{-2}) and the average 24-h air volume (24.0 m^{-3}) to convert elemental concentrations from ng cm^{-2} to ng m^{-3}.

2.2.3. Major ions

For the soluble ion analysis, one-quarter of each filter was cut and placed in a 5.0 mL polyethylene vial filled with deionized water, then rigorously shaken with an advanced digital VWR shaker (Model 5000 ADV 120 V) for 24-h and sonicated for 2-h using ultrasonic sonication. The extracted solutions were stored in a refrigerator at 4 °C before analysis with ion chromatography (ICS-3000, Dionex Corp., Sunnyvale, CA, USA). Anions (F^-, Cl^-, Br^-, NO_3^--N, SO_4^{2-}, and $C_2O_4^{2-}$) were separated using the Dionex ICS-3000 system with mixed eluent solutions of 8.0 mM sodium carbonate (Na_2CO_3) and 1.0 mM sodium bicarbonate ($NaHCO_3$). The instrument was equipped with a Dionex IonPac™ AS14 4*250 mm analytical column, AG14 4 mm guard column, 50.0 μL loop size, and a flow rate of 1.0 mL/min. Dionex Chromeleon software (version 6.60) was used to control the instrument, data acquisition, and chromatographic peak integration. A seven-point calibration (0.01, 0.02, 0.05, 0.10, 0.50, 0.80, and 1.0 mg/L for NO_3^--N, 0.02, 0.04, 0.10, 0.20, 1.0, 1.6, 2.0 mg/L for F^- and Br^-; and 0.10, 0.20, 0.50, 1.0, 5.0, 8.0, and 10.0 mg/L for Cl^-, SO_4^{2-} and $C_2O_4^{2-}$) was used. Samples for cations (Na^+, NH_4^+, K^+, Mg^{2+}, and Ca^{2+}) were analyzed with Dionex ICS-3000 using a CS16 5 mm analytical column, CG16 3 mm guard column, 25.0 μL loop size, 1.0 mL flow rate, and an eluent solution of 30 mM methanesulfonic acid (MSA). The calibration curves were determined using 0.10, 0.20, 0.50, 1.0, 5.0, 8.0, and 10.0 mg/L for the five cationic species.

The QC standard for the instrument calibration was achieved with Certified Analytical Reference Materials from the Environmental Research Agency (ERA), J.T.Baker, and NSI Laboratory Solutions at 5 mg/L with 0.9997 correlation coefficient and ± 10 % precision and accuracy (matrix spike and duplicate were 90 % - 110 % and ± 10 %, respectively). There were two reagent blanks analyzed at the beginning and the end of each calibration sequence and continuous calibration verification (CCV) standards (0.05 mg/L for NO_3^--N; 0.10 mg/L for F^- and Br^-; 0.50 mg/L for Cl^-, SO_4^{2-} and $C_2O_4^{2-}$). The minimum

reportable limit (MDL) was determined for each analyte as described in Lurie et al. (2019) and the MDL for all the analytes was 0.1 mg/L.

2.3. Source apportionment and transport of particles

The characterization of $PM_{2.5}$ and its constituents into sources was performed with a positive matrix factorization (PMF) model and the enrichment factor (EF). EF was calculated for excess concentration of trace metals in PM aerosols according to anthropogenic and natural sources. This tool has been used in studies to distinguish crustal material from anthropogenic elements and to determine the contribution of anthropogenic elements to the composition of elemental pollutants. The EF analysis used aluminum (Al) as a reference and followed the method described in Tao et al., 2013; Nayebare et al., 2016; Lurie et al., 2019; Moyebi, 2022.

The PMF model (version 5.0) was employed for the sources of $PM_{2.5}$ and its components. This model has been broadly used for source apportionment in several air pollution studies, and the result obtained in this study met all the functional criteria described in Nayebare et al., 2016, Lurie et al., 2019, and Moyebi, 2022. Prior information of elements serving as markers for $PM_{2.5}$ sources was employed in the identification of source profiles. For example, V and S served as markers for oil combustion, Ca, Al, Mg, Ti, Fe, K, and Si as markers for crustal elements, Na and Cl as markers for sea spray, BC and K as markers for biomass burning and vehicular emissions, and Ni, Cu, Zn, and Pb as markers for industrial as well as vehicular emissions. Five factors were identified for all the analytical runs in the base models and the runs were set at 20 with 100 % rate of convergence. After multiple runs of the model, the Q-true and Q-robust values were consistent, and the range was close. The concentration and uncertainty values were used to find the minimum Q-value, and species with <3 times the uncertainty values were excluded from the analysis.

Windrose plots and backward in-time trajectories were used to characterize the local and regional effects of wind speed and wind direction on both distribution and concentration of pollutants. The National Oceanic and Atmospheric Administration Hybrid Single-Particle Lagrangian Integrated Trajectory (HYSPLIT) model was used to determine the patterns of atmospheric particle transport for 72-h prior to the selected sampling days with high and low $PM_{2.5}$ concentrations at the Makro and KU sites. The backward in-time trajectory used the global data assimilation system with the isobaric vertical motion calculation method and a standard altitude above ground level set at 500 m. The total run time was set at 72-h with 6 new trajectories every 6-h and 4 maximum trajectories daily.

3. Results and discussion

3.1. Meteorological parameters

Table S1 summarizes the meteorological parameters during the entire length of the study and by season. The highest seasonal mean was observed in the spring for temperature (88 ± 2 °F) and in the summer for relative humidity (73 ± 6 %). The lowest seasonal mean for temperature (77 ± 6 °F) was recorded in the winter, while the lowest relative humidity (54 ± 15 %) was recorded in the fall. Daily temperature minimum and maximum values were 62 and 98 °F, and relative humidity values were 25 and 92 %, respectively.

3.2. Concentrations of $PM_{2.5}$ and its components

3.2.1. $PM_{2.5}$

The weekday-weekend temporal variations in $PM_{2.5}$ concentrations at the Makro and KU sites are reported in Table S2. $PM_{2.5}$ mass shows significant variability between the weekday and weekend at the two sites. Among the weekdays at the Makro site, the highest average $PM_{2.5}$ mass of 175 μg m^{-3} was on a Monday during a winter month, while the lowest was on a Wednesday (65.9 μg m^{-3}) in the summer. Meanwhile, the highest and lowest weekend average of 152 μg m^{-3} and 47.1 μg m^{-3} were recorded in the winter and spring, respectively. At the KU site, the highest weekday average of $PM_{2.5}$ was in the spring on a Thursday with 132 μg m^{-3}, while the highest weekend average (97.1 μg m^{-3}) was in the fall. The lowest weekday and weekend averages of $PM_{2.5}$ were in the summer (33.8 μg m^{-3}) and the spring (38.2 μg m^{-3}), respectively. This can be attributed to the vehicular traffic, which is considerably lower during the weekend. The weekday average emphasized the important role of anthropogenic activities in the elevation of $PM_{2.5}$ concentrations on workdays.

Table 1 shows the descriptive statistics for seasonal and annual $PM_{2.5}$ and BC concentrations at the Makro and KU sites. The highest $PM_{2.5}$ seasonal average concentrations at the Makro (136 ± 90.4 μg m^{-3}) and KU (92.0 ± 48.7 μg m^{-3}) sites were recorded in the winter and fall seasons, respectively. Higher mass concentrations were seen in all the four seasons at the Makro site compared to the KU site. The summer average at the Makro site (113 ± 187 μg m^{-3}) was almost triple (2.8-fold) that at the KU site (40.3 ± 15.9 μg m^{-3}). The lowest seasonal $PM_{2.5}$ mean concentrations were recorded in the spring (75.2 ± 45.5 μg m^{-3}) and the summer (40.3 ± 15.9 μg m^{-3}) at the Makro and KU sites, respectively. Significantly wide variations were observed between the lowest and highest concentrations in all the seasons at both sites. Elevated concentrations during the fall and winter seasons could be a result of several factors, such as meteorological conditions, low wind speed, low to stagnant air dispersion, and temperature inversion. The planetary boundary layer is usually lower in winter, which would explain the significantly high $PM_{2.5}$ concentrations. The annual $PM_{2.5}$ mass (daily average during the sampling period) at Makro (114 ± 115 μg m^{-3}) was almost double than that at KU (71.7 ± 56.4 μg m^{-3}).

Day-to-day and weekday/weekend variations are typically caused by human activities and environmental factors. Previous studies conducted in Karachi attributed diurnal changes to the intensity of industrial activity and day of the week (Khwaja et al., 2012; Lurie et al., 2019). Days with lower wind speed more often recorded maximum concentrations of $PM_{2.5}$ compared to days with high wind speeds (Lurie et al., 2019; Moyebi et al., 2022b).

Seasonal variation recorded in this study at the Makro site, with the highest levels in winter and lowest in summer agreed with other studies in areas with similar population and topography (Tao et al., 2013; Lurie et al., 2019; Rahman et al., 2019). High seasonal levels for fall and winter were consistent with a study conducted in Beijing, China, where levels of 65–105 μg m^{-3} and 80–110 μg m^{-3} were recorded in the fall and winter seasons, respectively (Guo et al., 2017). A study conducted on the total suspended particulate matter (TSP) in the twin cities of Pakistan between December 1998 and January 1999 reported high average concentrations of TSP in Karachi (668 μg m^{-3}) and Islamabad (691 μg m^{-3}) (Parekh et al., 2001). Surprisingly, Nayebare et al. (2018) found seasonal $PM_{2.5}$ variations with high spring (113 ± 67.1 μg m^{-3}) and low winter (67.6 ± 36.9 μg m^{-3}) average values in Makkah, Saudi Arabia, which was suggested to be due to the climate conditions. The annual mean recorded in this study at the Makro site was comparable to other data reported in air pollution studies (Krzyzanowski et al., 2014; Song et al., 2018; Rahman et al., 2020), and higher than the mean concentration observed at an industrial/residential site in Karachi (101 ± 45.6 μg m^{-3}) by Lurie et al. (2019). Khwaja et al. (2012) reported that Karachi's $PM_{2.5}$ concentration was among the highest in the world consistent with the levels in this study. A study by Ma et al.'s (2019) in the Yangtze River Delta region in China found that the contribution of land and sea breezes, favorable meteorological conditions, mixing and dilution effects, and low emissions affected $PM_{2.5}$ concentrations.

Air pollution studies have shown that $PM_{2.5}$ increases during the winter or cool season due to high emission of pollutants from biomass burning, fossil fuel use, and space/house heating coupled with lower mixing layer height, including thermal inversion (Squizzato et al., 2018). Numerous emission sources such as coal, wood, and agricultural waste burned to generate heat greatly influence the higher levels of $PM_{2.5}$ in winter (Cheng et al., 2016). Higher boundary layer height and unfavorable meteorological conditions such as high precipitation and high wind speed also reduce the concentration of $PM_{2.5}$ in summer (Ma et al., 2019).

Table 1
Descriptive statistics depicting seasonal and annual means of $PM_{2.5}$ and BC at the Makro and KU sites during the study period.

			$PM_{2.5}$ (μg m^{-3})				BC (μg m^{-3})		
Site	Season	N	Mean ± SD	Min.	Max.	N	Mean ± SD	Min.	Max.
Makro	Oct.-Nov. 2009	44	134 ± 72.7	36.3	395	44	4.51 ± 2.55	0.52	10.2
	Feb.-Mar. 2010	45	136 ± 90.4	8.4	435	43	3.67 ± 2.28	0.05	12.2
	April–June 2010	45	75.2 ± 45.5	35.8	309	44	2.76 ± 0.88	1.38	7.04
	July-Aug. 2010	45	113 ± 187	51	1206	45	2.63 ± 0.89	0.92	6.35
	Annual	179	114 ± 115	8.4	1206	176	3.39 ± 1.97	0.05	12.2
KU	Oct.-Nov. 2009	45	92.0 ± 48.7	46.2	326	45	4.64 ± 1.90	2.25	10.8
	Feb.-Mar. 2010	43	81.8 ± 31.5	24.7	159	43	3.98 ± 1.42	1.65	7.18
	April–June 2010	44	73.2 ± 87.4	24	475	44	1.20 ± 0.58	0.42	3.98
	July-Aug. 2010	45	40.3 ± 15.9	22	115	44	0.96 ± 0.46	0.26	2.46
	Annual	177	71.7 ± 56.4	22	475	176	2.70 ± 2.06	0.26	10.8

Note: Oct.-Nov. 2009 (Fall), Feb.-Mar. 2010 (Winter), April–June 2010 (Spring), and July-Aug. 2010 (Summer).

3.2.2. Black carbon

BC in Karachi, believed to be mostly emitted from heavy-duty diesel vehicles, was found in concentrations ranging from 0.05 to 12.2 μg m^{-3} (Makro) and 0.26–10.8 μg m^{-3} (KU) (Table 1). Maximum daily BC concentrations at the Makro and KU sites were observed during the winter (12.2 μg m^{-3}) and fall (10.8 μg m^{-3}) seasons, respectively. Seasonal BC concentrations were high in the fall and winter at both sites with low daily variations in the spring and summer.

Time of the day is another important factor to consider in BC concentrations. Heavy vehicular emissions, use of industrial power generators, and levels of industrial operations can significantly impact daily levels of BC in urban areas. BC concentrations are generally high during morning and evening rush hours, and during work hours when traffic flow is at the peak (Moyebi et al., 2022b). In a study conducted at the Port of Albany, New York (USA), the maximum concentration (11.9 μg m^{-3}) recorded was consistent with this study. This is due to combustion of fossil fuel and diesel emitted from trucks around the sampled site (Moyebi et al., 2022b). The annual average BC concentrations in this study (Makro = 3.39 ± 1.97 μg m^{-3}; KU = 2.70 ± 2.06 μg m^{-3}) agrees with other major cities worldwide such as Athens (2.44 ± 0.66 μg m^{-3}; Grivas et al., 2019), Hong Kong (3.2 ± 0.9 μg m^{-3}; Zhang et al., 2018), Istanbul (2.76 ± 1.97 μg m^{-3}; Kuzu et al., 2020), Beijing (3.27 μg m^{-3}; Liu et al., 2016), and Karachi (3.44 ± 1.93 μg m^{-3}; Lurie et al., 2019). BC levels in Karachi in the winter (Makro = 3.67 ± 2.28 μg m^{-3}; KU = 3.98 ± 1.42 μg m^{-3}) and summer (Makro = 2.63 ± 0.89 μg m^{-3}; KU = 0.96 ± 0.46 μg m^{-3}) were comparable to the values in major cities of Asia such as Tehran (winter = 3.5 μg m^{-3}; summer = 3.5 μg m^{-3}) (Esmaeilirad et al., 2020) and Shanghai (winter = 2.88 ± 2.03 μg m^{-3}; summer = 0.84.5 ± 0.46 μg m^{-3}) (Ming et al., 2017).

3.2.3. Trace metals

Metals were categorized based on their possible sources into sea spray, vehicular and industrial emissions, crustal material, and oil combustion. A total of 28 and 19 trace metals were quantified at the Makro and KU sites, respectively (Tables 2, 3, and S3). At the Makro site (Table 2), the most abundant metals were in the decreasing order of Ca (12,722 ± 17,691 ng m^{-3}) > Si (5853 ± 4958 ng m^{-3}) > S (5,129 ± 3784 ng m^{-3}) > Pb (4962 ± 11,324 ng m^{-3}) > Cl (3808 ± 2525 ng m^{-3}) > Zn (3511 ±

Table 2
Summary statistics of seasonal average concentrations of trace metals (ng m^{-3}) at the Makro site during the study period in Karachi, Pakistan.

Metals		Oct.-Nov. 2009				Feb.-Mar. 2010				April–June 2010				July-Aug. 2010		
(ng/m^3)	N	Mean ± SD	Min.	Max.	N	Mean ± SD	Min.	Max.	N	Mean ± SD	Min.	Max.	N	Mean ± SD	Min.	Max.
Pb	44	14,374 ± 18,388	118	92,505	45	4569 ± 6510	39.7	26,698	45	249 ± 352	39.2	2219	42	573 ± 1259	58.3	6382
Ca	44	8752 ± 6418	3071	43,810	45	20,240 ± 19,389	870	87,676	45	9335 ± 9062	1585	56,265	42	12,456 ± 26,232	2752	137,209
S	44	8190 ± 4950	2727	27,696	45	5369 ± 2899	68.6	14,044	45	3750 ± 1552	1063	11,224	42	3145 ± 2629	1571	17,600
Zn	44	7466 ± 7590	618	33,048	45	3198 ± 3471	10.8	16,050	45	779 ± 411	119	1856	42	2629 ± 1636	461	6520
Si	44	4877 ± 2520	2188	16,375	45	8598 ± 6061	293	26,292	45	5286 ± 4108	1118	20,801	42	4541 ± 5271	1192	30,805
Fe	44	3371 ± 2047	1172	11,511	45	4811 ± 3639	208	17,438	45	2564 ± 2072	741	11,997	42	3040 ± 5233	909	27,440
Na	44	2980 ± 2101	630	9096	45	1802 ± 1107	50.7	6264	45	1943 ± 578	928	3864	42	3155 ± 805	1662	4575
Cl	43	2538 ± 2368	156	10,989	45	2342 ± 1060	29.6	4318	45	3791 ± 1823	393	7542	42	6699 ± 1935	1851	10,296
K	44	2299 ± 1462	530	6094	45	2002 ± 1184	77.6	5320	45	1138 ± 681	427	3879	42	1182 ± 1166	529	6858
Al	44	1673 ± 952	642	6045	45	2881 ± 2140	657	9843	45	1694 ± 1518	195	7325	42	1449 ± 1541	454	9347
Mg	44	813 ± 378	327	2343	45	1175 ± 811	20.7	3906	45	926 ± 478	310	2699	42	889 ± 439	327	3025
Y	44	485 ± 624	3.81	3161	43	162 ± 221	2.66	890	42	9.76 ± 12.7	1.12	77.9	41	21.2 ± 42.5	2.78	207
Sb	22	351 ± 274	95.7	1305	ND	ND	ND	ND	ND	ND	ND	ND	ND	ND	ND	ND
Br	42	306 ± 314	41.8	1438	43	190 ± 189	47.3	1152	45	81.8 ± 34.7	33.5	204	42	118 ± 56.2	35.1	277
Sn	29	247 ± 152	67.5	685	ND	ND	ND	ND	ND	ND	ND	ND	ND	ND	ND	ND
Ti	44	213 ± 115	87.3	639	45	381 ± 277	19.0	1329	45	227 ± 177	65.4	972	42	237 ± 385	80.5	2055
Mn	44	158 ± 133	31.3	534	45	159 ± 131	5.52	591	45	70.0 ± 53.8	16.9	318	42	90.1 ± 129	37.0	687
Cu	44	158 ± 169	11.7	761	45	94.1 ± 77.3	6.13	376	45	28.7 ± 20.1	7.23	131	42	49.1 ± 37.8	11.2	196
Lu	44	156 ± 94.1	45.1	433	45	142 ± 88	3.31	408	45	73.3 ± 35.9	22.9	244	42	100 ± 90.5	44.9	501
Er	44	148 ± 101	38.8	479	44	151 ± 104	39.5	470	45	68.2 ± 44.2	13.8	284	42	99.2 ± 111	45.4	593
W	44	126 ± 142	9.49	645	38	68.6 ± 59.5	8.78	248	ND	ND	ND	ND	22	29.1 ± 16.0	7.46	68.7
Zr	28	89.9 ± 75.8	18.3	366	22	58.3 ± 28.4	25.3	127	ND	ND	ND	ND	ND	ND	ND	ND
Ir	25	53.2 ± 35.6	11.7	158	ND	ND	ND	ND	ND	ND	ND	ND	ND	ND	ND	ND
Ni	44	48.1 ± 24.3	20.1	130	45	51.8 ± 31.6	0.71	154	45	31.5 ± 15.4	10.7	101	42	35.3 ± 37.1	18.5	202
Sr	44	41.9 ± 30.9	14.9	207	45	88.4 ± 81.2	2.85	361	45	47.0 ± 39.4	12.4	246	42	61.5 ± 130	14.7	654
Cr	44	27.3 ± 23.8	6.13	136	44	34.3 ± 30.8	2.79	125	45	15.6 ± 16.2	2.05	101	41	19.8 ± 45.9	4.20	240
Rb	23	8.40 ± 6.30	1.88	27.2	39	11.1 ± 7.72	2.78	32.4	27	6.32 ± 4.97	2.21	21.6	22	8.93 ± 14.5	2.68	55.4
P	ND	ND	ND	ND	38	211 ± 253	6.70	1122	37	81.2 ± 99.4	17.1	571	36	147 ± 326	20.3	1605

Note: Oct.-Nov. 2009 (Fall), Feb.-Mar. 2010 (Winter), April–June 2010 (Spring), and July-Aug.(Summer). <ND (not determined).

Table 3
Summary statistics of seasonal average concentrations of trace metals (ng m^{-3}) at the KU site during the study period in Karachi, Pakistan.

Metals		Oct.-Nov. 2009				Feb.-Mar. 2010				April–June 2010				July-Aug. 2010		
(ng/m^3)	N	Mean ± SD	Min.	Max.	N	Mean ± SD	Min.	Max.	N	Mean ± SD	Min.	Max.	N	Mean ± SD	Min.	Max.
Na	45	2532 ± 1145	490	6844	43	3136 ± 1163	767	6008	44	4967 ± 1797	1513	9740	45	8232 ± 1793	2791	12,477
Mg	45	1693 ± 895	600	5159	43	2428 ± 1552	452	8947	44	2317 ± 1316	771	7472	45	1783 ± 626	708	3321
Al	35	1982 ± 1314	644	6503	23	2590 ± 2056	424	9980	43	1910 ± 1989	179	12,294	44	980 ± 465	354	2584
Si	45	5053 ± 2802	1152	15,639	43	7193 ± 4141	1313	23,392	44	4960 ± 4945	681	31,017	45	2462 ± 1070	912	5882
S	45	6813 ± 1861	3293	11,457	43	5707 ± 2125	2143	12,139	44	3819 ± 1613	1473	12,653	45	3135 ± 963	1416	5805
K	45	2258 ± 1360	743	6601	43	1674 ± 821	520	3843	44	877 ± 857	268	5972	45	658 ± 205	358	1194
Ca	45	5621 ± 2643	2196	12,411	43	6042 ± 2865	1188	13,641	44	4582 ± 7456	850	50,416	45	2200 ± 794	687	4681
Ti	45	166 ± 82.1	54.2	495	43	231 ± 125	45.6	730	44	167 ± 211	25.1	1430	45	84.1 ± 30.2	32.2	171
V	45	30.7 ± 18.9	7.87	97.3	43	38.2 ± 19.4	7.71	84.1	44	29.4 ± 16.5	<DL	95.4	44	20.9 ± 11.8	5.14	51.8
Cr	45	7.99 ± 3.06	2.98	17.1	43	11.9 ± 7.23	3.33	39.6	44	8.71 ± 12.0	<DL	79.4	45	5.46 ± 6.30	<DL	36.2
Mn	45	71.3 ± 28.0	24.4	143	43	91.1 ± 48.2	10.4	226	44	45.8 ± 69.8	5.02	480	44	43.0 ± 47.6	7.25	285
Fe	45	2075 ± 879	653	5390	43	2715 ± 1373	464	8099	44	1876 ± 2704	268	18,426	45	1043 ± 474	377	2397
Co	44	0.40 ± 0.22	<DL	1.00	43	0.63 ± 0.41	<DL	1.99	34	0.45 ± 0.73	<DL	4.40	30	0.20 ± 0.13	<DL	0.47
Ni	45	9.69 ± 6.26	4.16	45.3	43	11.0 ± 3.71	3.64	17.6	44	9.55 ± 5.32	2.16	37.0	45	8.33 ± 11.0	2.10	78.6
Cu	45	53.0 ± 33.8	12.6	198	43	42.4 ± 21.6	7.10	113	44	23.1 ± 21.9	5.33	146	44	24.2 ± 17.6	5.58	97.5
Zn	45	969 ± 750	131	3708	43	1255 ± 982	59.8	5295	44	414 ± 295	52.5	1513	45	884 ± 685	69.1	3565
Pb	45	5029 ± 4714	71.8	20,706	43	6447 ± 6424	61.8	21,446	44	707 ± 942	<DL	4298	45	867 ± 1054	43.5	3835
As	44	1.92 ± 0.83	<DL	4.17	43	2.14 ± 1.15	0.81	5.68	43	1.02 ± 0.52	<DL	2.08	44	1.39 ± 2.57	<DL	18.0
Cl	45	872 ± 558	97.2	2610	43	1203 ± 520	148	2372	44	1849 ± 1012	326	5305	45	2826 ± 1075	353	4934

Note: Oct.-Nov. 2009 (Fall), Feb.-Mar. 2010 (Winter), April–June 2010 (Spring), and July-Aug.(Summer). <ND (not determined) and < DL (less than the detection limits).

4918 ng m^{-3}). The major trace metals at the KU site (Table 3) were in the order of Si (4891 ± 3915 ng m^{-3}) > S (4,865 ± 2243 ng m^{-3}) > Na (4733 ± 2694 ng m^{-3}) > Ca (4595 ± 4470 ng m^{-3}) > Pb (3241 ± 4745 ng m^{-3}). Currently, there are no regulated standards for metals in Pakistan. There are significant health risks associated with the major trace metals, and for which WHO guidelines are available. For example, V is a potent respiratory irritant, Cr, Ni, and As are of concern owing to their carcinogenicity, Mn leads to increased risk of neuro-behavioral function, and Pb is a potent neurotoxin. It is notable that levels of Cr, Mn Ni, As, and Pb in this study exceeded the recommended WHO limits (Table 4). The crustal elements that are mainly attributed to urban dust/soil resuspension were present at high concentrations at the Makro and KU sites. Other anthropogenic elements such as Pb, S, and Zn were also high at the Makro and KU sites. The sea spray elements (Na and Cl) were high in the summer, with average concentrations of 3155 ± 805 and 6699 ± 1935 ng m^{-3} at the Makro site and 8232 ± 1793 and 2826 ± 1075 ng m^{-3} at the KU site due to the sea breeze from the Arabian Sea. The influence of the sea breeze was determined by calculating the annual and summer average ratios of Na:Cl. Summer average of Na:Cl ratios were 0.47 at Makro and 2.91 at KU with annual average ratios of 0.65 at Makro and 2.80 at the KU site. The ratio observed at the Makro site suggests the influence of wind from the Arabian sea, while the ratio at the KU site indicates Na sources.

The concentrations of trace metals in this study were extremely high. Elevated concentration of the crustal elements can be due to periodical sandstorms and strong wind currents that result in soil/dust resuspension, which was evident in the concentrations of crustal elements during a dust storm reported in Tao et al. (2013). Several studies have found crustal and anthropogenic elements as part of $PM_{2.5}$ chemical composition with the sources being resuspension of dust, traffic emissions, combustion of oil/fossil fuels, and industrial emissions (Tao et al., 2013; Salameh et al., 2015; Nayebare et al., 2018; Lurie et al., 2019; Moryani et al., 2020). The average ratio of Na:Cl recorded at the Makro site was consistent with the ratio reported at the Korangi site (0.71), while the KU ratio was >2 times greater than that at the Tibet Center (1.2) with both the Makro and KU sites exceeding the ratio found in pure seawater (Lurie et al., 2019). This indicates potential depletion of atmospheric chlorine.

Table 4
Comparison of levels of trace metals concentrations with WHO guidelines (μg m^{-3}) for $PM_{2.5}$.

Toxic metals	Makro	KU	WHO
V	–	0.002–0.097	1
Cr	0.002–0.24	0.0006–0.079	0.000025[a]
Mn	0.005–0.69	0.005–0.48	0.15
Ni	0.0007–0.20	0.002–0.079	0.0025
As	–	0.00002–0.018	0.00066[a]
Pb	0.04–92	0.011–21	0.5

[a] For a risk of 1:1,000,000.

3.2.4. Ionic species

3.2.4.1. Anions. Seasonal and annual water-soluble anions (F^-, Cl^-, Br^-, NO_3^-, and SO_4^{2-}) are presented in Table S4. The maximum concentrations of F^- (2.99 μg m^{-3}), and Br^- (0.17 μg m^{-3}) were recorded in the winter at the Makro site, while F^- (0.43 μg m^{-3}), and Br^- (0.44 μg m^{-3}) were observed in the summer at the KU site. NO_3^--N concentrations ranged from 0.19 to 2.01 μg m^{-3} (Makro) and 0.10–1.69 μg m^{-3} (KU). Cl^- and SO_4^{2-} concentrations were consistently high at both sites in all the seasons with the highest seasonal mean of SO_4^{2-} (7.29 ± 6.63 and 11.0 ± 3.29 μg m^{-3}) observed in the fall, while Cl^- seasonal average concentrations (4.91 ± 1.64 and 2.90 ± 1.37 μg m^{-3}) were highest in the summer at the Makro and KU sites.

3.2.4.2. Cations. Table S5 shows the summary of the seasonal and annual water-soluble cations (Na^+, NH_4^+, K^+, Mg^{2+}, and Ca^{2+}) at the Makro and KU sites. Na^+ and Ca^{2+} dominated the water-soluble fraction and steadily increased in all the seasons. The water-solution fraction of Na^+ was recorded at high average concentrations in summer at the Makro (3.76 ± 1.38 μg m^{-3}) and KU (2.44 ± 0.84 μg m^{-3}) sites. The increase in Na^+ and Ca^{2+} again confirmed the contribution of marine aerosols from the Arabian Sea. NH_4^+ was not found in more than half of the total samples at both sites, suggesting that NH_4^+ concentration is low in urban centers with no major agricultural activities where NH_4^+ fertilizer and mechanized farm tools are widely used.

Ionic species (Na^+ and Cl^-) that are associated with sea spray were high in the summer, which suggested that winds from the Arabian Sea are a significant source of sea spray elements in Karachi. This was consistent with Lurie et al. (2019) who reported high Na^+ and Cl^- in the summer. Na^+ and Ca^{2+} levels were also found to increase in rural and coastal sites with Na^+ attributed to sea salt aerosols while Ca^{2+} was due to soil dust (Mmari et al., 2013). Nayebare et al. (2016) observed higher SO_4^{2-} levels than NO_3^- in Rabigh with SO_4^{2-} concentrations comparable to this study. Tian et al. (2018) reported a lower fraction of NO_3^- in the spring, which agreed with the observed low level of NO_3^- in this study and may be due to low relative humidity resulting in weaker chemical process. NH_4^+ concentrations were low at both sites and were lower than values reported in

a study conducted in Cairo, where values ranged from 2.3 to 6.3 μg m^{-3} in the winter and 3.5–12.6 μg m^{-3} in the summer (Hassan et al., 2013).

3.3. Comparison with WHO and other studies in developed and developing countries

The average annual $PM_{2.5}$ concentrations observed at the Makro and KU sites were compared with the WHO guidelines and studies conducted in urban centers in developed and developing countries across the world (Fig. 2). Annual $PM_{2.5}$ average concentrations significantly exceeded the WHO guideline (5 μg m^{-3}) by factors of 22.8 and 14.3 at the Makro and KU sites, respectively. Also, >99 % of the daily $PM_{2.5}$ concentrations exceeded the WHO 24-h guideline (15 μg m^{-3}) by a factor of 9 at the Makro site and were 6 times higher at the KU site. The Makro site (Karachi) recorded a higher annual mean concentration (114 ± 115 μg m^{-3}) than what was previously reported at Korangi – Karachi (101 ± 45.6 μg m^{-3}) (Lurie et al., 2019). The annual concentration in this study was one of the highest $PM_{2.5}$ levels reported in the world, similar to other Asian cities with poor air quality problems. Asian cities like Delhi, India and Dhaka, Bangladesh recorded higher $PM_{2.5}$ levels of 169 μg m^{-3} and 135 μg m^{-3}, respectively, while Chengdu, China recorded 165 μg m^{-3} (Tao et al., 2013; Krzyzanowski et al., 2014). The comparison showed that $PM_{2.5}$ concentrations were extremely high in the developing countries but relatively lower in the developed countries.

3.4. Correlation matrix

Table S6 (Makro) and S7 (KU) show the intercorrelation between $PM_{2.5}$, BC, trace metals, ionic species, and meteorological parameters at the Makro and KU sites. $PM_{2.5}$ was moderately correlated with temperature at the Makro (r = 0.399, p-value = 0.0066) and KU (r = 0.402, p-value = 0.0075) sites in the winter.

$PM_{2.5}$ was highly correlated with BC (r > 0.600, p-value <0.0001) in three out of the four seasons at both sites suggesting significant contribution from vehicular emissions to $PM_{2.5}$ levels. $PM_{2.5}$ had moderate to very high correlations (r = 0.300 to >0.700, p-value <0.05) with crustal elements (Mg, Al, Si, K, Ca, Mn, Fe, and Ni) in the fall, and very high correlations ($r \geq 0.80$, p-value <0.0001) in the winter and spring at the Makro site. Also, the intercorrelation between the crustal elements was very high. High correlations were observed between $PM_{2.5}$ (r > 0.600, p-value <0.0001) and other elements (S, Zn, Pb, Cl, Sb, Na, Sn, and NH_4^+) from anthropogenic sources.

At the KU site, $PM_{2.5}$ was highly correlated with K (r = 0.587, p-value <0.0001) and NO_3^- (r = 0.618, p-value <0.0001), and moderately correlated (r > 0.30, p-value <0.05) with S, Ca, Mn, Fe, F^-, and Br^- in the fall. In the winter, spring, and summer seasons, $PM_{2.5}$ had high to very high correlations with crustal elements (Mg, Si, K, Ca, Mn, Fe, and Ni). Other elements including water-soluble elements that correlated with $PM_{2.5}$ were S, Zn, Pb, V, Cl, F^-, and NO_3^-.

Cross-site Pearson correlations and coefficients of divergence (COD) calculations were performed to determine homogeneity of $PM_{2.5}$ levels measured at both sites (Table 5). The COD was calculated using the equation (Xue et al., 2010):

$$COD_{AB} = \sqrt{\frac{1}{p}\sum_{i=1}^{p}\left(\frac{x_{Ai}-x_{Bi}}{x_{Ai}+x_{Bi}}\right)^2}$$ where A and B are two different sites, x_{Ai} is the i^{th} averaged concentration of $PM_{2.5}$ measured at site A (Makro), x_{Bi} is the i^{th} averaged concentration of $PM_{2.5}$ measured at site B (KU), and p is the number of observations.

The COD values in all the seasons were >0.2, indicating that there was no homogeneity in sources of $PM_{2.5}$ levels at the Makro and KU sites. This shows that the sources and transport of ambient PM between the two sites were heterogeneous.

3.5. Source apportionment and particle transport

Source characterization of ambient air pollution is a critical part of determining the chemical composition in order to appropriately identify, regulate and control the sources that greatly contribute to the poor air quality.

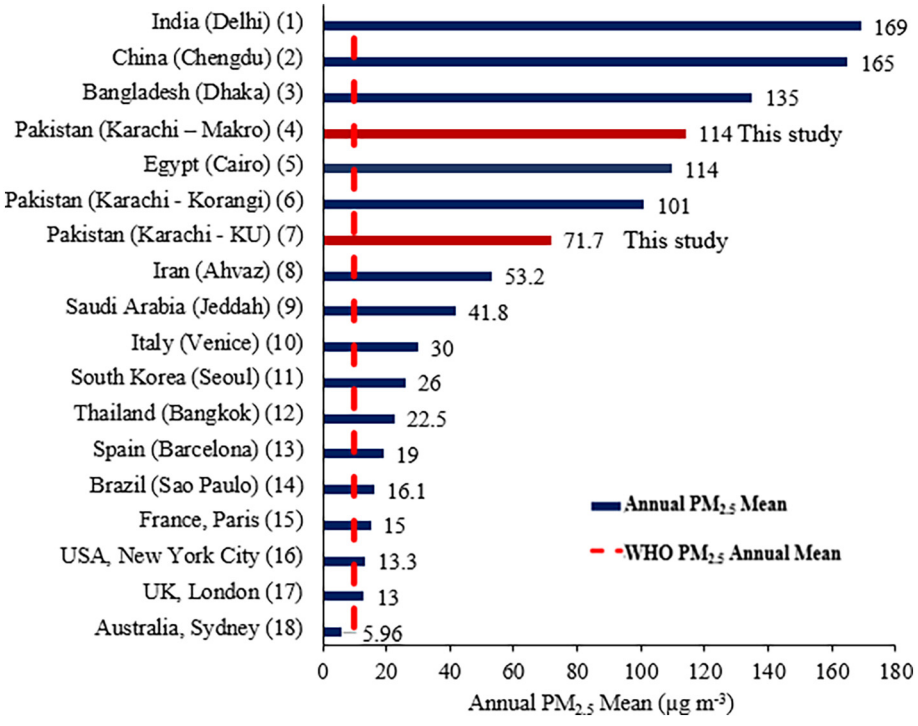

Fig. 2. Comparison of annual $PM_{2.5}$ mean concentrations measured in Karachi (Makro and KU sites) with the WHO and average annual concentrations reported in cities in developed and developing countries.
(1,3) Krzyzanowski et al., 2014; (2) Tao et al., 2013; (4,7)* This study; (5) Cheng et al., 2016; (6) Lurie et al., 2019; (8) Sicard et al., 2019; (9) Khwaja et al.- unpublished; (10,13) Salameh et al., 2015; (11) Park and Ko, 2018; (12) Narita et al., 2019; (14) Andreão et al., 2018; (15) Bressi et al., 2013; (16) Squizzato et al., 2018; (17) Pascal et al., 2013; (18) Chang et al., 2019.

Table 5
Pearson cross-site correlation and coefficient of divergence (COD) for $PM_{2.5}$ between the Makro and KU sites.

Season	r	COD
Oct.-Nov. 2009	0.307**	0.27
Feb.-Mar. 2010	0.475	0.29
April–June 2010	0.322**	0.23
July-Aug. 2010	−0.172*	0.33
Annual	0.135**	0.28

** p-value < 0.0001.
* p-value < 0.05.

This section is divided into source characterization (EF and PMF) and particle transport (wind rose and backward-in-time trajectories).

3.5.1. Enrichment factor (EF)

Fig. 3 shows the EF analysis for the sources of trace metals. The values for the relative abundance of trace metals in the earth crust were obtained from Taylor (1964). Al was used as a reference element to account for the contribution of anthropogenic activities to air pollution using the equation:

$$EF = \frac{(C_x/C_{Al})_{Aerosol}}{(C_x/C_{Al})_{Earth\ Crust}}$$

where C_x = concentration of the examined analyte (element X) in the PM aerosol and earth crust C_{Al} = concentration of the reference element (Al) in the PM aerosol and earth crust.

Trace metals with log EF values greater than one represent anthropogenic sources while a log EF value less than one suggests natural sources. The estimation of EF values for the Makro and KU sites support the substantial influence of anthropogenic sources on the levels of trace metals. Trace metals with annual average log EF values of more than one at the Makro site were Ca, Ni, Cu, Y, S, Cl, Sn, W, Zn, Br, Lu, Pb, and Sb. Some of the metals had log EF values ranging from 1.5 to 4.5, signifying enormous anthropogenic contribution to the PM aerosol. At the KU site, eight metals (V, Na, Cu, As, Zn, Cl, S, and Pb) had log EF values greater than one. Results confirmed that S, Zn, Pb, Cu, and Cl consistently had log EF values greater than one at both sites.

The EF analysis was a confirmatory tool in the classification of natural and anthropogenic air pollutant sources. It was observed that the crustal elements (Ca, Si, Fe, Al, Mg, K, and Ti) were mainly associated with soil resuspension rather than anthropogenic emissions, which is consistent with data reported in other studies (Tao et al., 2013; Nayebare et al., 2018; Tian et al., 2018). Ca, a crustal element with EF log >1 at the Makro site could have been due to contribution from cement dust and road/building construction being an industrial/residential site. Tian et al. (2018) found an association between Ca and rapid development/construction in Tianjin, China. Zn, Ni, S, Cu, and Pb have been found to have EF values corresponding to anthropogenic sources in other studies that used the EF analysis for source apportionment (Nayebare et al., 2016; Lurie et al., 2019; Moryani et al., 2020).

3.5.2. Positive matrix factorization (PMF)

The source profile and factor contributions to air pollutants are illustrated in Fig. 4a (Makro site) and Fig. 4b (KU site).

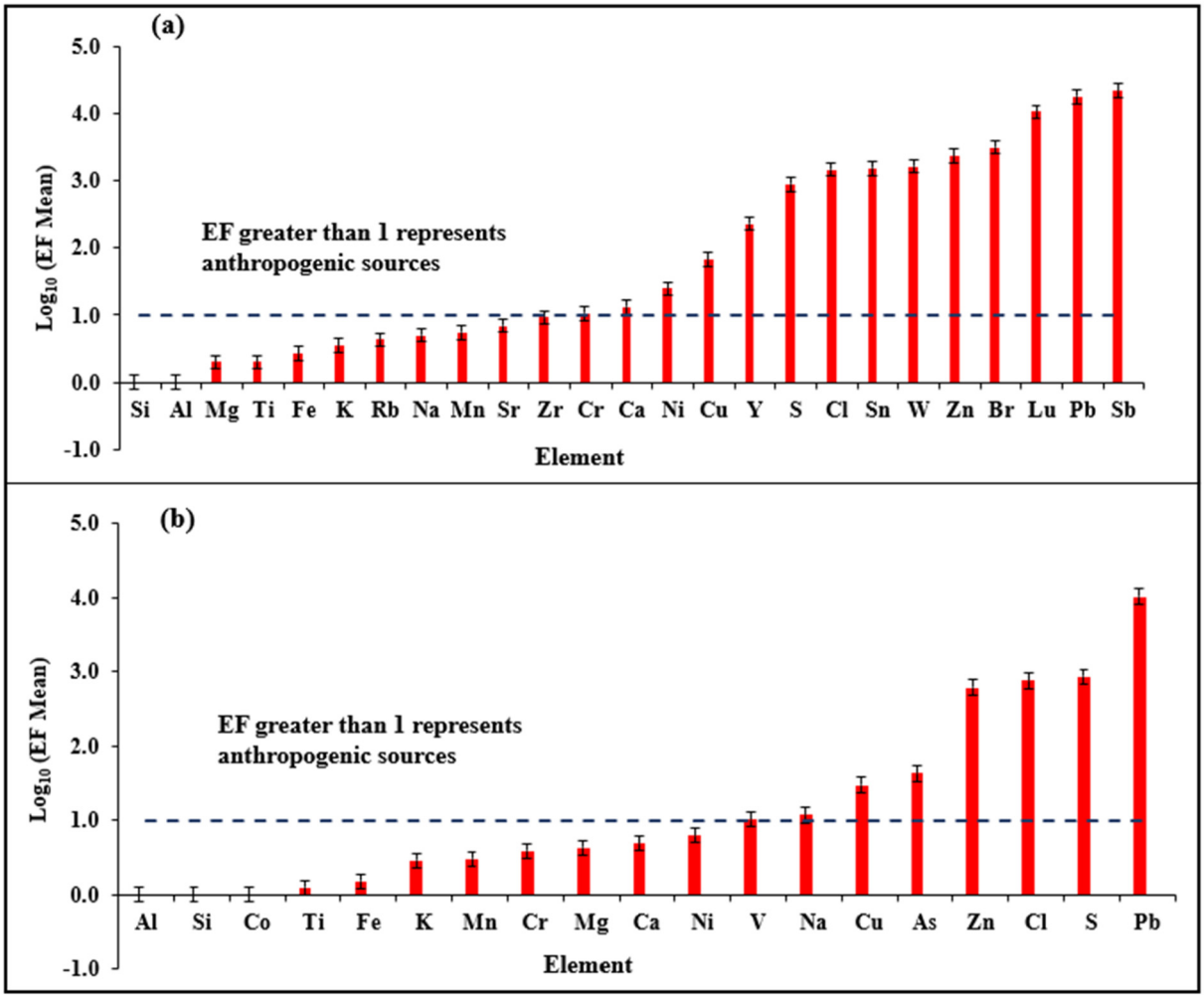

Fig. 3. Enrichment factor (EF) log transformed for measured trace metals at the Makro (a) and KU (b) sites during the study period.

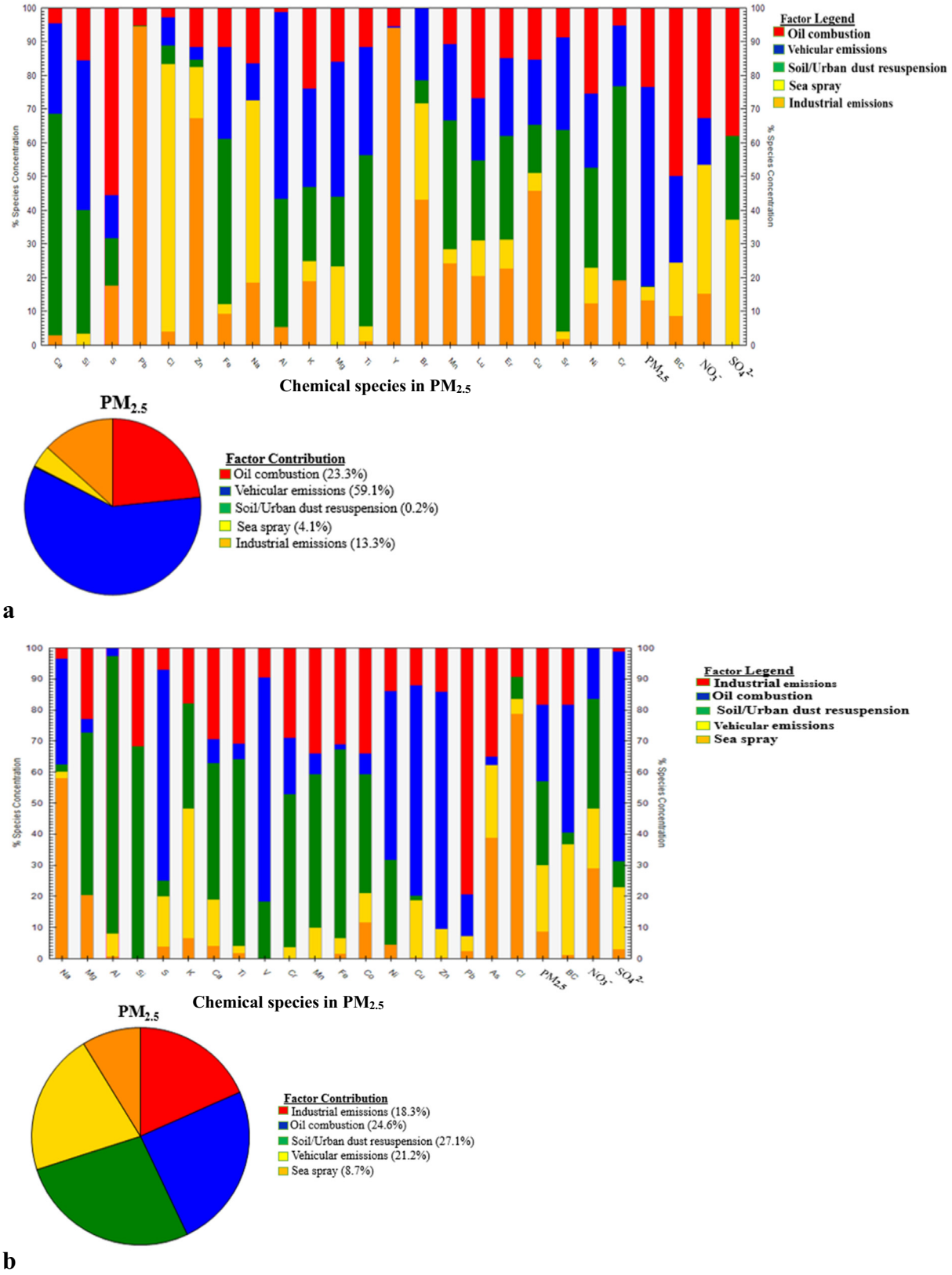

Fig. 4. Positive matrix factorization factor fingerprint profiles and factor contribution to $PM_{2.5}$ concentration at the Makro (a) and KU (b) sites.

The first factor, with a similar overall contribution to $PM_{2.5}$ at the Makro (59.1 %) and KU (21.2 %) sites was vehicular emissions, which contributed highly to the factor profiles of BC, Si, S, Zn, K, Ca, NO_3^-, SO_4^{2-}, Fe, Na, Mg, Ti, Mn, Cu, Pb, Ni, Cr, Lu, Er, As, and Sr. Air pollutants that are released from the automobiles are from the incomplete fuel combustion, tires, brake pads, and engine oils (Sharma et al., 2016; Nayebare et al., 2018; Lurie et al., 2019). Some of the metals that were categorized as anthropogenic by the EF analysis were found to be associated with vehicular

emissions by the PMF source profile contribution. NO_3^- and SO_4^{2-} formed by the gas-phase photochemical reaction and as a by-product of combustion activities generally constitutes the secondary fraction of $PM_{2.5}$ aerosol.

The second factor that contributed to the $PM_{2.5}$ levels at Makro (23.3 %) and KU (24.6 %) was oil combustion, which contributed to the factor profiles of S, Pb, Zn, Y, V, Ni, Br, Cu, Lu, K, Mn, Na, Er, Cr, BC, NO_3^-, and SO_4^{2-}. Metals that are mainly associated with oil combustion are S, Zn, V, Y, and Ni (Lurie et al., 2019). Fossil fuel naturally contains V as an impurity while S produced by industrial combustion-related activities is emitted in the form of sulfur dioxide (Lurie et al., 2019). Some of the elements present in oil combustion such as Pb, Ni and Zn are used as anti-knock agents, additives and/or catalysts in engine oil and other industrial processes (Parekh et al., 2002; Hussain et al., 2018; Lurie et al., 2019).

The third factor was industrial emissions, which contributed 13.3 % and 18.3 % to $PM_{2.5}$ levels at the Makro and KU sites, respectively. Industrial emissions significantly contributed to the factor profiles of Mg, Si, K, Ca, Ti, S, Cr, Br, Mn, Fe, Lu, Er, Co, Pb, V, NO_3^-, As, Zn, Ni, Al, Cu, SO_4^{2-}, Sr, and BC. Emissions from battery manufacturing, smelters, brake repair in automobiles, construction and repair industry, industrial and petrochemical plants, cement industry, and diesel-powered industrial operations confirm the extremely high concentrations of some of the metals such as Pb, Ni, Zn, Ca, Si, and Fe found in this category (Mohmand et al., 2015; Sharma et al., 2016; Nayebare et al., 2018; Tian et al., 2018; Qadeer et al., 2020).

The fourth and fifth factors were soil or urban dust resuspension and sea spray. These two factors were shown to contribute 27.1 % and 8.7 % to $PM_{2.5}$ levels at the KU site but contributed only 0.2 % and 4.1 % to $PM_{2.5}$ concentrations at the Makro site. The soil/urban dust resuspension contributed to the factor profiles of the crustal elements (Ca, Ti, Al, K, Mg, Si, and Fe,) (Tao et al., 2013; Nayebare et al., 2018; Tian et al., 2018). The profile of K may have been influenced by the constant open biomass burning (Tian et al., 2018), which is very common in Karachi. In addition, other anthropogenic elements with contributions from soil/urban dust resuspension to their factor profiles were Mn, Sr, S, Lu, Er, NO_3^-, Cu, Ni, Cr, Co, Cl, V, and SO_4^{2-}. The fifth factor was the sea spray, which was known to largely contribute to the factor profiles of Na and Cl at both sites and also contributed to the profiles of other sea salt elements (Mg and K) (Sharma et al., 2016) as well as NO_3^-, SO_4^{2-}, Br, As, S, Co, Zn, Mn, Lu, Ni, and Er.

3.5.3. Wind rose

The wind rose plots showing the influence of wind speed and wind direction are presented in Fig. S1. Wind rose plots typically explain the local contribution of wind speed on the levels of $PM_{2.5}$. $PM_{2.5}$ seasonal concentrations increase with decreasing wind speed in the fall and winter. Maximum average concentrations of $PM_{2.5}$ were recorded in the fall and winter seasons at the Makro site (Table 1) when about 60 % of the wind speeds were <11 mph. The lowest $PM_{2.5}$ average concentration was recorded in the spring with wind speeds rising as high as 20 mph. At the KU site, the same inverse relationship occurred in the fall, which had the highest $PM_{2.5}$ mean and lowest wind speeds. Summer season at the KU site had the lowest observed $PM_{2.5}$ average concentrations and higher wind speeds in the upper limits, some above 20 mph. The variation in the seasonal $PM_{2.5}$ levels at both sites was in part a result of the localized effect of wind speeds, which increases the atmospheric dispersion in seasons with minimum $PM_{2.5}$ concentrations, especially in the spring and summer when the boundary layer is also high.

3.5.4. Backward-in-time trajectories

The 72-h backward-in-time trajectories were performed to show the impact of wind direction and transport of particles on high and low daily $PM_{2.5}$ concentrations per season (Fig. S2a and S2b). The high $PM_{2.5}$ concentration recorded on November 6, 2009 corresponds with a wind direction from the north that blew over the industrial inland area to the sampling site. The wind direction in the winter and spring seasons on March 6 and April 30, 2010 corresponding with high $PM_{2.5}$ concentrations mainly came from the northwest (Fig. S2a). Low concentrations of $PM_{2.5}$ recorded on February 28, 2010 occurred with the wind direction from the south and southwest blowing over the Arabian Sea. $PM_{2.5}$ concentrations resulting from sea breezes are usually lower due to the dilution effect. At the KU sampling site (Fig. S2b), the maximum $PM_{2.5}$ levels were recorded on days with wind trajectories that followed the same pattern observed at the Makro site. Wind trajectories for high $PM_{2.5}$ concentrations mostly blew from inland, passing over the busy M.A. Jinnah Road, with over 300, 000 automobiles passing daily, and through a heavily industrialized part of Karachi, thus transporting particles emitted from traffic, biomass burning, industrial processes, and other human activities to the sampling area.

3.6. Air quality index (AQI)

AQI proportion was calculated for daily $PM_{2.5}$ levels per season to measure the quality of the air at the Makro and KU sites (Fig. 5). AQI has six categories of index values and levels of concern, which are *good* (0–50), *moderate* (51–100), *unhealthy for sensitive population groups* (101–150), *unhealthy* (151–200), *very unhealthy* (201 − 300), and *hazardous* (301 and above) (EPA). This study calculates the percentage of each index value based on the measured $PM_{2.5}$ concentrations at Makro and KU sites. Higher AQI values indicate poor air quality and levels of health concern in Karachi. None of the four cycles at the Makro site recorded a single day with good or moderate air quality. >66 % of the air quality levels at the Makro site were *unhealthy* in all the seasons, while *very unhealthy* and *hazardous* AQI levels were recorded in the fall (20.5 %) and winter (13.6 %), respectively. At the KU site, *moderate* AQI levels were recorded in the winter and summer, while the AQI level for *very unhealthy* was 34.1 % in the spring. The AQI in the fall and winter at the Makro and KU sites had about 68 % atmospheric air reported to be *unhealthy* for the general population. These results are a clear indication of the poor air quality in Karachi.

3.7. Risk and health impact assessment

The human health risk and impact assessment of $PM_{2.5}$ were calculated for short-term exposure using the Risk Assessment Information System. The estimation of human health impact assessment for risk of exposure and expected number of deaths were calculated using the following equations (https://rais.ornl.gov/tutorials/tutorial.html):

$$\text{Risk} = \text{CDI X SF (mg/kg/day)}$$

$$\text{CDI} = \Big[\text{Concentration of } PM_{2.5}(\text{mg/m}^3) \times \text{IR}(\text{m}^3/\text{hour}) \times \text{ET}(\text{hours/event}) \times \text{EF}(\text{days/year}) \times \text{ED}(\text{years})\Big] \div [\text{BW}(\text{kg}) \times \text{AT}(\text{day/year}) \times \text{LT}(\text{years})]$$

where CDI = chronic daily intake, SF = slope factor, IR = inhalation rate; ET = exposure time; EF = exposure frequency; ED = exposure duration; BW = body weight; AT = average time; LT = lifetime. IR was assumed at 0.625 m^3/h, SF = 1.1 mg/kg/day, ET = 12 h/event, EF = 365 days/year, ED = 30 years, BW = 70 kg, AT = 365 days/year, and the LT = 70 years.

The expected number of deaths were estimated with the formula:

$$E = \beta \times B \times P \times C$$

where E is the expected number of deaths, β is the percent change in mortality per 10 μg/m^3 (0.004), B is the incidence of the deaths per 1000 people (0.0071), P is exposed population (13,386,730), and C is the change in pollutant concentration (μg/m^3 × 0.1). $PM_{2.5}$ concentrations were averaged for annual and seasonal exposure risks in order to calculate the chronic daily intake. The annual risks were estimated at 0.0058 (Makro) and 0.0036 (KU) per 1000 (Fig. 6). The seasonal inhalation risks per 1000 due to short-term exposure in the fall, winter, spring, and summer seasons were 0.0068, 0.0069, 0.0038, and 0.0057 at the Makro site, while the risks were 0.0047, 0.0041, 0.0037, and 0.0020 at the KU site.

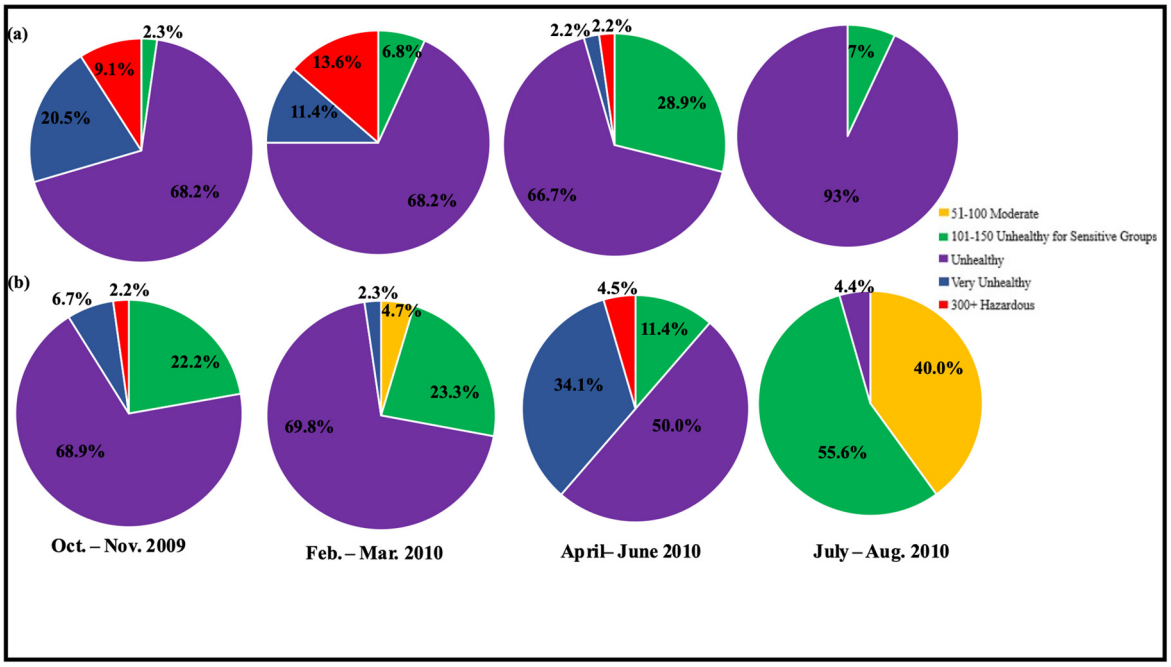

Fig. 5. Air Quality Index (AQI) for $PM_{2.5}$ concentrations at Makro (a) and KU (b) sites during the study period based on seasonal 24-h averages.

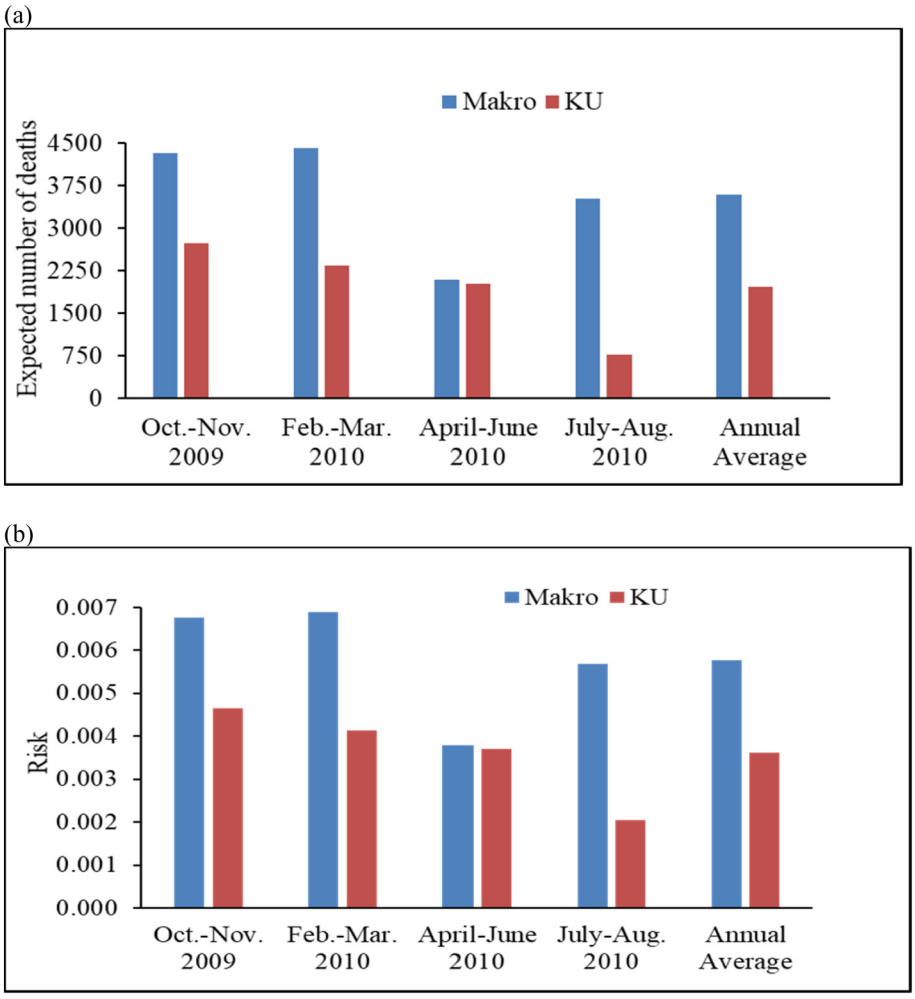

Fig. 6. Human health impact assessment for expected number of deaths due to short-term exposure to $PM_{2.5}$ (a) and risk per 1000 people (b) for seasonal and annual chronic inhalation.

The expected number of deaths attributable to seasonal and annual $PM_{2.5}$ exposure at the Makro and KU sites for all ages and genders are presented in Fig. 6. The Makro site had a higher estimated number of expected deaths resulting from short-term exposure to $PM_{2.5}$ than the KU site in all the seasons as well as the annual average. The estimated number of deaths were higher in the fall and winter seasons at the Makro (4329 and 4425) and KU (2739 and 2348) sites. The annual estimates of the expected number of deaths were 3592 at the Makro site and 1971 at the KU site. Seasons with the highest average $PM_{2.5}$ concentrations at Makro (winter) and KU (fall), as previously observed in Table 1, recorded the highest expected number of deaths.

4. Conclusions

The air quality in Karachi is extremely poor and greatly exceeds the WHO daily and annual guidelines as well as the $PM_{2.5}$ levels from many megacities in the world. Results of this study indicate that the primary anthropogenic sources of air pollution in Karachi were industrial activities, traffic emissions, and fossil fuel combustion. High concentrations were recorded in some crustal (Ca, Si, and Fe) and anthropogenic (Ni, Cu, S, Sn, Zn, Lu, Pb, and Sb) elements. AQI data confirmed the human health impact of poor daily air quality, which was generally rated *unhealthy* for the general population. Estimated risk assessment and expected number of deaths due to inhalation of $PM_{2.5}$ were high in the fall and winter, and higher at the Makro (industrial/residential site) by about a factor of 1.8 than at the KU site without major industrial activity.

Data from this study provide vital information needed by policy makers to design targeted and cost-effective regulations on $PM_{2.5}$ emissions in major cities of Pakistan. The information produced from this crucial study can be used to focus attention on improving emission records for sources revealed to be significant contributors to ambient air pollution, and to begin to consider how possible emission control strategies might affect air quality.

Furthermore, the government of Pakistan needs to put in place control measures capable of improving the air quality in Karachi by enforcing annual vehicle inspection and emission control, placing a cap on sulfur dioxide release and industrial emissions, regulating open biomass or waste burning, and developing public mass transit in major cities of Pakistan to reduce the number of vehicles on the road. Considering the poor ambient air pollution observed in this study, it is recommended that residents wear masks and spend less time outdoor to help mitigate the risk of exposure to toxic air pollutants.

Data availability

The authors confirm that the data supporting the findings of this study are available within the article and the posted supplementary data.

Declaration of competing interest

The authors declare that they have no known competing financial interests or personal relationships that could have appeared to influence the work reported in this paper.

Acknowledgements

The authors would like to thank the Wadsworth Center, New York State Department of Health, University at Albany, Higher Education Commission, Pakistan, and University of Karachi. The sites were made available for the project courtesy of Dr. Aftab Turabi. We are grateful to the Center for Applied Nuclear Science and Technology, National Nuclear Energy Agency of Indonesia and Department of Environmental Medicine, and the NYU School of Medicine for the technical support. We are indebted to Ms. Kelly Robbins and Drs. Vincent Dutkiewicz and Sumayya Saied who assisted us in all aspects of this work. We extend our thanks to Dr. Kim McClive-Reed for editing the manuscript.

Funding

This work was funded by the Pakistan-US Science and Technology Cooperative Program (administered by National Academy of Sciences) under grant # PGA-7251-07-010.

Consent for publication

All authors agree to the publication in this journal.

CRediT authorship contribution statement

Haider A. Khwaja, Conceptualization; Omosehin D. Moyebi, Jahan Zeb, Azhar Siddique, Data curation; Omosehin D. Moyebi and Mirza M. Hussain, Formal analysis; Zafar Fatmi, Azhar Siddique, and Kamran Khan, Methodology; Haider A. Khwaja and David O. Carpenter, Project administration; David O. Carpenter, Muhayatun Santoso, and Mirza M. Hussain, Resources; Omosehin D. Moyebi, Software; Haider A. Khwaja, Supervision; Omosehin D. Moyebi, Writing—original draft; Haider A. Khwaja and David O. Carpenter, Writing—review and editing. All authors have read and agreed to the published version of the manuscript.

Appendix A. Supplementary data

Supplementary data to this article can be found online at https://doi.org/10.1016/j.scitotenv.2023.161474.

References

Andreão, W.L., Albuquerque, T.T.A., Kumar, P., 2018. Excess deaths associated with fine particulate matter in Brazilian cities. Atmos. Environ. 194, 71–81. https://doi.org/10.1016/j.atmosenv.2018.09.034.

Anjum, M.S., Ali, S.M., Imad-Ud-Din, M., Subhani, M.A., Anwar, M.N., Nizami, A.S., Ashraf, U., Khokhar, M.F., 2021. An emerged challenge of air pollution and ever-increasing particulate matter in PakistanA critical review. J. Hazard. Mater. 402, 123943. https://doi.org/10.1016/j.jhazmat.2020.123943.

Barletta, B., Meinardi, S., Simpson, I.J., Khwaja, H.A., Blake, D.R., Rowland, F.S., 2002. Mixing ratios of volatile organic compounds (VOCs) in the atmosphere of KarachiPakistan. Atmos. Environ. 36 (21), 3429–3443.

Bloomberg CityLab, 2020. The world's worst public transport system attempts to modernize. Available online: https://www.bloomberg.com/news/features/2020-11-02/pakistan-s-megacity-tries-to-modernize (accessed on November 3, 2020).

Bressi, M., Sciare, J., Ghersi, V., Bonnaire, N., Nicolas, J.B., Petit, J.-E., Moukhtar, S., Rosso, A., Mihalopoulos, N., Féron, A., 2013. A one-year comprehensive chemical characterization of fine aerosol ($PM_{2.5}$) at urban, suburban and rural background sites in the region of Paris (France). Atmos. Chem. Phys. 13 (15), 7825–7844. https://doi.org/10.5194/acp-13-7825-2013.

Chang, L.T.-C., Scorgie, Y., Duc, H.N., Monk, K., Fuchs, D., Trieu, T., 2019. Major source contributions to ambient PM2.5 and exposures within the New South Wales greater metropolitan region. Atmosphere 10, 138. https://doi.org/10.3390/atmos10030138.

Cheng, Z., Luo, L., Wang, S., Wang, Y., Sharma, S., Shimadera, H., Wang, X., Bressi, M., de Miranda, R.M., Jiang, J., Zhou, W., Fajardo, O., Yan, N., Hao, J., 2016. Status and characteristics of ambient PM2.5 pollution in global megacities. Environ. Int. 89 (90), 212–221. https://doi.org/10.1016/j.envint.2016.02.003.

Cohen, D.D., Crawford, J., Stelcer, E., Bac, V.T., 2010. Characterization and source apportionment of fine particulate sources at Hanoi from 2001 to 2008. Atmos. Environ. 44, 320–328. https://doi.org/10.1016/j.atmosenv.2009.10.037.

EPA, n.d.EPA (Environmental Protection Agency) (n.d.). AirNow. https://www.airnow.gov/aqi/aqi-basics/ (accessed 18 April 2020).

Esmaeilirad, S., Lai, A., Abbaszade, G., Schnelle-Kreis, J., Zimmermann, R., Uzu, G., Daellenbach, K., Canonaco, F., Hassankhany, H., Arhami, M., Baltensperger, U., 2020. Source apportionment of fine particulate matter in a middle eastern Metropolis, Tehran-Iran, using PMF with organic and inorganic markers. Sci. Total Environ. 705, 135330.

Grivas, G., Stavroulas, I., Liakakou, E., Kaskaoutis, D.G., Bougiatioti, A., Paraskevopoulou, D., Gerasopoulos, E., Mihalopoulos, N., 2019. Measuring the spatial variability of black carbon in Athens during wintertime. Air Qual. Atmos. Health 12 (12), 1405–1417.

Guo, H., Wang, Y., Zhang, H., 2017. Characterization of criteria air pollutants in Beijing during 2014–2015. Environ. Res. 154, 334–344. https://doi.org/10.1016/j.envres.2017.01.029.

Gurung, A., Bell, M.L., 2013. The state of scientific evidence on air pollution and human health in Nepal. Environ. Res. 124, 54–64. https://doi.org/10.1016/j.envres.2013.03.007.

Hassan, S.K., El-Abssawy, A.A., Khoder, M.I., 2013. Characteristics of gas–phase nitric acid and ammonium–nitrate– sulfate aerosol, and their gas–phase precursors in a suburban area in Cairo, Egypt. Atmos. Pollut. Res. 4, 117–129. https://doi.org/10.5094/APR.2013.012.

Hussain, M., Akhtar, F., Khan, S.S., 2018. Impact and ratio of lead in ambient air from vehicular emission in Quetta Valley, Pakistan. IOP conference series. Mater. Sci. Eng. 414 (1). https://doi.org/10.1088/1757-899X/414/1/012044.

IARC (International Agency for Research on Cancer), 2016. Outdoor Air Pollution: IARC Monographs on the Evaluation of Carcinogenic Risks to Humans. 109 Lyon, France.
Khwaja, H.A., Fatmi, Z., Malashock, D., Aminov, Z., Siddique, A., Carpenter, D.O., 2012. Effect of air pollution on daily morbidity in KarachiPakistan. J. Local Glob. Health Sci. 3. https://doi.org/10.5339/jlghs.2012.3.
Krzyzanowski, M., Apte, J.S., Bonjour, S.P., Brauer, M., Cohen, A.J., Pruss-Ustun, A., 2014. Air pollution in the mega-cities. Curr. Environ. Health Rep. 1, 185–191. https://doi.org/10.1007/s40572-014-0019-7.
Kumar, P., Druckman, A., Gallagher, J., Gatersleben, B., Allison, S., Eisenman, T.S., Hoang, U., Hama, S., Tiwari, A., Sharma, A., Abhijith, K.V., Adlakha, D., McNabola, A., Astell-Burt, T., Feng, X., Skeldon, A.C., de Lusignan, S., Morawska, L., 2019. The nexus between air pollution, green infrastructure and human health. Environ. Int. 133 (Pt A), 105181. https://doi.org/10.1016/j.envint.2019.105181.
Kuzu, S.L., Yavuz, E., Akyüz, E., Saral, A., Akkoyunlu, B.O., Özdemir, H., Demir, G., Ünal, A., 2020. Black carbon and size-segregated elemental carbon, organic carbon compositions in a megacity: a case study for Istanbul. Air Qual. Atmos. Health 13 (7), 827–837.
Lebbie, T.S., Moyebi, O.D., Asante, K.A., Fobil, J., Brune-Drisse, M.N., Suk, W.A., Sly, P.D., Gorman, J., Carpenter, D.O., 2021. E-waste in Africa: a serious threat to the health of children. Int. J. Environ. Res. Public Health 18, 8488. https://doi.org/10.3390/ijerph18168488.
Liu, Q., Ma, T., Olson, M.R., Liu, Y., Zhang, T., Wu, Y., Schauer, J.J., 2016. Temporal variations of black carbon during haze and non-haze days in Beijing. Sci. Rep. 6 (1), 1–10.
Lurie, K., Nayebare, S.R., Fatmi, Z., Carpenter, D.O., Siddique, A., Malashock, D., Khan, K., Zeb, J., Hussain, M.M., Khatib, F., Khwaja, H.A., 2019. PM2.5 in a megacity of Asia (Karachi): source apportionment and health effects. Atmos. Environ. 202, 223–233. https://doi.org/10.1016/j.atmosenv.2019.01.008.
Ma, T., Duan, F., He, K., Qin, Y., Tong, D., Geng, G., Liu, X., Li, H., Yang, S., Ye, S., Xu, B., Zhang, Q., Ma, Y., 2019. Air pollution characteristics and their relationship with emissions and meteorology in the Yangtze River Delta region during 2014–2016. J. Environ. Sci. 83, 8–20. https://doi.org/10.1016/j.jes.2019.02.031.
Malashock, D., Khwaja, H., Fatmi, Z., Siddique, A., Lu, Y., Lin, S., Carpenter, D., 2018. Short-term association between black carbon exposure and cardiovascular diseases in Pakistan's largest megacity. Atmosphere 9, 420. https://doi.org/10.3390/atmos9110420.
Ming, L., Jin, L., Li, J., Fu, P., Yang, W., Liu, D., Zhang, G., Wang, Z., Li, X., 2017. PM2. 5 in the Yangtze River Delta, China: chemical compositions, seasonal variations, and regional pollution events. Environ. Pollut. 223, 200–212.
Mmari, A.G., Potgieter-Vermaak, S.S., Bencs, L., McCrindle, R.I., Grieken, R.V., 2013. Elemental and ionic components of atmospheric aerosols and associated gaseous pollutants in and near Dar Es SalaamTanzania. Atmos. Environ. 77, 51–61. https://doi.org/10.1016/j.atmosenv.2013.04.061.
Mohmand, J., Eqani, S.A., Fasola, M., Alamdar, A., Mustafa, I., Ali, N., Liu, L., Peng, S., Shen, H., 2015. Human exposure to toxic metals via contaminated dust: bio-accumulation trends and their potential risk estimation. Chemosphere 132, 142–151. https://doi.org/10.1016/j.chemosphere.2015.03.004.
Moryani, H.T., Kong, S., Du, J., Bao, J., 2020. Health risk assessment of heavy metals accumulated on PM2.5 fractioned road dust from two cities of Pakistan. Int. J. Environ. Res. Public Health 17 (19), 7124. https://doi.org/10.3390/ijerph17197124.
Moyebi, O.D., 2022. Megacity: A Reservoir of Toxic Environmental Contaminants and Health Disease Burden (Publication No. 29162526). Doctoral DissertationUniversity at Albany ProQuest Dissertations and Theses Global.
Moyebi, O.D., Frank, B.P., Tang, S., LaDuke, G., Carpenter, D.O., Khwaja, H.A., 2022b. Ambient size-segregated particulate matter characterization from a port in upstate New York. Atmosphere 13 (6), 984. https://doi.org/10.3390/atmos13060984.
Narita, D., Oanh, N.T.K., Sato, K., Huo, M., Permadi, D.A., Chi, N.N.H., Ratanajaratroj, T., Pawarmart, I., 2019. Pollution characteristics and policy actions on fine particulate matter in a growing Asian economy: The case of Bangkok Metropolitan Region. Atmosphere 10, 227. https://doi.org/10.3390/atmos10050227.
Nayebare, S.R., Aburizaiza, O.S., Khwaja, H.A., Siddique, A., Hussain, M.M., Zeb, J., Khatid, F., Carpenter, D.O., Blake, D.R., 2016. Chemical characterization and source apportionment of PM2.5 in rabighSaudi Arabia. Aerosol Air Qual Res. 16, 3114–3129. https://doi.org/10.4209/aaqr.2015.11.0658.
Nayebare, S.R., Aburizaiza, O.S., Siddique, A., Carpenter, D.O., Hussain, M.M., Zeb, J., Aburiziza, A.J., Khwaja, H.A., 2018. Ambient air quality in the holy city of Makkah: A source apportionment with elemental enrichment factors (EFs) and factor analysis (PMF). Environ. Pollut. (Barking, Essex: 1987) 243 (Pt B), 1791–1801. https://doi.org/10.1016/j.envpol.2018.09.086.
NIST (National Institute of Standards and Technology), 2019. .Available online: https://www.nist.gov/laboratories/tools-instruments/instrumental-neutron-activation-analysis-inaa (accessed 2 December 2019).
Omanga, E., Ulmer, L., Berhane, Z., Gatari, M., 2014. Industrial air pollution rural Kenya: community awareness, risk perception and associations between risk variables. BMC Public Health 14, 377. https://doi.org/10.1186/1471-2458-14-377.
Pangaribuan, M., Chuang, K., Chuang, H., 2019. Association between exposures to air pollution and biomarkers of cardiovascular disease in northern Taiwan. Atmos. Pollut. Res. 10 (4), 1250–1259. https://doi.org/10.1016/j.apr.2019.02.008.
Parekh, P.P., Khwaja, H.A., Khan, A.R., Naqvi, R.R., Malik, A., Shah, S.A., Khan, K., Hussain, G., 2001. Ambient air quality of two metropolitan cities of Pakistan and its health implications. Atmos. Environ. 35, 5971–5978 S1352-2310(00)00569-0.
Parekh, P.P., Khwaja, H.A., Khan, A.R., Naqvi, R.R., Malik, A., Khan, K., Hussain, G., 2002. Lead content of petrol and diesel and its assessment in an urban environment. Environ. Monit. Assess. 74 (3), 255–262. https://doi.org/10.1023/a:1014296713553.
Park, S.-H., Ko, D.-W., 2018. Investigating the effects of the built environment on $PM_{2.5}$ and PM_{10}: A case study of Seoul Metropolitan City, South Korea. Sustainability 10, 4552. https://doi.org/10.3390/su10124552.
Pascal, M., Corso, M., Chanel, O., Declercq, C., Badaloni, C., et al., 2013. Assessing the public health impacts of urban air pollution in 25 European cities: results of the Aphekom project. Sci. Tot. Environ. 449, 390–400. https://doi.org/10.1016/j.scitotenv.2013.01.077.
Phosri, A., Ueda, K., Phung, V., Tawatsupa, B., Honda, A., Takanoa, H., 2018. Effects of ambient air pollution on daily hospital admissions for respiratory and cardiovascular diseases in BangkokThailand. Sci. Total Environ. 651, 1144–1163. https://doi.org/10.1016/j.scitotenv.2018.09.183.
Pope 3rd, C.A., Dockery, D.W., 2013. Air pollution and life expectancy in China and beyond. PNAS USA 110 (32), 12861–12862. https://doi.org/10.1073/pnas.1310925110.
Qadeer, A., Saqib, Z.A., Ajmal, Z., Xing, C., Khalil, S.K., Usman, M., Huang, Y., Bashir, S., Ahmad, Z., Ahmed, S., Thebo, K.H., Liu, M., 2020. Concentrations, pollution indices and health risk assessment of heavy metals in road dust from two urbanized cities of Pakistan: comparing two sampling methods for heavy metals concentration. Sustain. Cities Soc. 53, 101959. https://doi.org/10.1016/j.scs.2019.101959.
Rahman, M.M., Mahamud, S., Thurston, G.D., 2019. Recent spatial gradients and time trends in Dhaka, Bangladesh, air pollution and their human health implications. J. Air Waste Manag. Assoc. 69 (4), 478–501. https://doi.org/10.1080/10962247.2018.1548388.
Rahman, M.M., Begum, B.A., Hopke, P.K., Nahar, K., Thurston, G.D., 2020. Assessing the PM2.5 impact of biomass combustion in megacity Dhaka, Bangladesh. Environ. Pollut. 264, 114798. https://doi.org/10.1016/j.envpol.2020.114798.
Rajak, R., Chattopadhyay, A., 2020. Short and long term exposure to ambient air pollution and impact on health in India: a systematic review. Int. J. Environ. Health Res. 30 (6), 593–617. https://doi.org/10.1080/09603123.2019.1612042.
Salameh, D., Detournay, A., Pey, J., Pérez, N., Liguori, F., Saraga, D., Bove, M.C., Brotto, P., Cassola, F., Massabò, D., Latella, A., Pillon, S., Formenton, G., Patti, S., Armengaud, A., Piga, D., Jaffrezo, J.L., Bartzis, J., Tolis, E., Prati, P., Querol, X., Worthman, H., Marchand, N., 2015. PM2.5 chemical composition in five European Mediterranean cities: a 1-year study. Atmos. Res. 155, 102–117. https://doi.org/10.1016/j.atmosres.2014.12.001.
Sharma, S.K., Mandal, T.K., Jain, S., Saraswati, Sharma, A., Saxena, M., 2016. Source apportionment of PM2.5 in Delhi, India using PMF model. Bull. Environ. Contam. Toxicol. 97 (2), 286–293. https://doi.org/10.1007/s00128-016-1836-1.
Sicard, P., Khaniabadi, Y.O., Perez, S., Gualtieri, M., De Marco, A., 2019. Effect of O_3, PM_{10} and $PM_{2.5}$ on cardiovascular and respiratory diseases in cities of France, Iran and Italy. Environ. Sci. Poll. Res. 26 (31), 32645–32665. https://doi.org/10.1007/s11356-019-06445-8.
Simpson, I.J., Aburizaiza, O.S., Siddique, A., Barletta, B., Blake, N.J., Gartner, A., Khwaja, H., Meinardi, S., Zeb, J., Blake, D.R., 2014. Air quality in Mecca and surrounding holy places in Saudi Arabia during hajj: initial survey. Environ. Sci. Technol. 48 (15), 8529–8537. https://doi.org/10.1021/es5017476.
Soleimani, M., Akbari, N., Saffari, B., Haghshenas, H., 2022. Health effect assessment of PM2.5 pollution due to vehicular traffic (case study: Isfahan). J. Transp. Health 24, 101329. https://doi.org/10.1016/j.jth.2022.101329.
Song, J., Zheng, L., Lu, M., Gui, L., Xu, D., Wu, W., Liu, Y., 2018. Acute effects of ambient particulate matter pollution on hospital admissions for mental and behavioral disorders: a time-series study in ShijiazhuangChina. Sci. Total Environ. 636, 205–211. https://doi.org/10.1016/j.scitotenv.2018.04.187.
Squizzato, S., Masiol, M., Rich, D.Q., Hopke, P.K., 2018. PM2.5 and gaseous pollutants in New York state during 2005–2016: spatial variability, temporal trends, and economic influences. Atmos. Environ. 183, 209–224. https://doi.org/10.1016/j.atmosenv.2018.03.045.
State of Global Air, 2018. Region & city PM2.5 ranking.Available online: https://www.stateofglobalair.org/sites/default/files/soga-2018-report.pdf (accessed on December 23, 2019).
Tao, J., Zhang, L., Engling, G., Zhang, R., Yang, Y., Cao, J., Zhu, C., Wang, Q., Luo, L., 2013. Chemical composition of PM2.5 in an urban environment in Chengdu, China: importance of springtime dust storms and biomass burning. Atmos. Res. 122, 270–283. https://doi.org/10.1016/j.atmosres.2012.11.004.
Taylor, S.R., 1964. Abundance of chemical elements in the continental crust: a new table. Geochim. Cosmochim. Acta 28 (8), 1273–1285.
Tian, Y., Liu, J., Han, S., Shi, X., Shi, G., Xu, H., Yu, H., Zhang, Y., Feng, Y., Russell, A.G., 2018. Spatial, seasonal and diurnal patterns in physicochemical characteristics and sources of PM2.5 in both inland and coastal regions within a megacity in China. J. Hazard. Mater. 342, 139–149. https://doi.org/10.1016/j.jhazmat.2017.08.015.
WHO (World Health Organization), 2018. Air pollution and child health: prescribing clean air summary; World Health Organization: Geneva, Switzerland, 2018.Available online: https://apps.who.int/iris/handle/10665/275545 accessed on November 25, 2019.
Wu, Y., Zhang, S., Hao, J., Liu, H., Wu, X., Hu, J., Walsh, M.P., Wallington, T.J., Zhang, K.M., Stevanovic, S., 2017. On-road vehicle emissions and their control in China: a review and outlook. Sci. Total Environ. 574, 332–349. https://doi.org/10.1016/j.scitotenv.2016.09.040.
Xia, S.Y., Huang, D.S., Jia, H., Zhao, Y., Li, N., Mao, M.Q., Lin, H., Li, Y.X., He, W., Zhao, L., 2019. Relationship between atmospheric pollutants and risk of death caused by cardiovascular and respiratory diseases and malignant tumors in Shenyang, China, from 2013 to 2016: an ecological research. Chin. Med. J. 132 (19), 2269–2277. https://doi.org/10.1097/CM9.0000000000000453.
Xue, Y., Wu, J., Feng, Y., Dai, L., Bi, X., Li, X., Li, X., Zhu, T., Tang, S., Chen, M., 2010. Source characterization and apportionment of PM10 in Panzhihua, China. Aerosol Air Qual Res. 10, 367–377. https://doi.org/10.4209/aaqr.2010.01.0002.
Yang, B., Guo, Y., Markevych, I., Qian, Z., Bloom, M.S., Heinrich, J., Dharmage, S.C., Rolling, C.A., Jordan, S.S., Kompula, M., Leskinen, A., Bowatte, G., Li, S., Chen, G., Liu, K., Zeng, X., Hu, L., Dong, G., 2019. Association of long-term exposure to ambient air pollutants with risk factors for cardiovascular disease in China. JAMA Netw. Open 2 (3), e190318. https://doi.org/10.1001/jamanetworkopen.2019.0318.
Zhang, Q., Shen, Z., Ning, Z., Wang, Q., Cao, J., Lei, Y., Sun, J., Zeng, Y., Westerdahl, D., Wang, X., Wang, L., Xu, H., 2018. Characteristics and source apportionment of winter black carbon aerosols in two chinese megacities of Xi'an and Hong Kong. Environ. Sci. Pollut. Res. Int. 25 (33), 33783–33793. https://doi.org/10.1007/s11356-018-3309-z.
Zou, X., Azam, M., Islam, T., Zaman, K., 2015. Environment and air pollution like gun and bullet for low-income countries: war for better health and wealth. Environ. Sci. Pollut. Res. 23 (4), 3641–3657. https://doi.org/10.1007/s11356-015-5591-3.